



Contents lists available at ScienceDirect

Gondwana Research

journal homepage: www.elsevier.com/locate/gr

Madagascar volcanic provinces linked to the Gondwana break-up: Geochemical and isotopic evidences for contrasting mantle sources

Jacques-Marie Bardintzeff^{a,b,*}, Jean-Paul Liégeois^c, Bernard Bonin^a,
Hervé Bellon^d, Georges Rasamimanana^{a,e}

^a Laboratoire de Pétrographie-Volcanologie, UMR CNRS IDES 8148, Bât. 504, Université Paris-Sud, 91405 Orsay Cédex, France

^b IUFM, Université de Cergy-Pontoise, 95000 Cergy-Pontoise, France

^c Isotope Geology, Royal Museum for Central Africa, B-3080 Tervuren, Belgium

^d UMR 6538 Domaines océaniques, IUEM, Université de Bretagne Occidentale, Université européenne de Bretagne, 6 av. Le Gorgeu, CS 93837, 29238 Brest Cédex 3, France

^e Ministère de l'Energie et des Mines, BP 322, Ampandrianomby, 101 Antananarivo, Madagascar

ARTICLE INFO

Article history:

Received 15 July 2008

Received in revised form 12 November 2009

Accepted 16 November 2009

Available online xxx

Keywords:

Madagascar

K–Ar geochronology

Sr–Nd isotopes

Mantle source

Hot spot

ABSTRACT

After the Gondwana break-up and Greater India splitting off, Madagascar suffered volcanic episodes. The Cretaceous Morondava flood basalt (CFB) province was emplaced ca. 93 Ma ago. Two coeval high-Ti–P (HTP) and low-Ti–P (LTP) suites are distributed within the alkaline Ankilizato (central) and tholeiitic Manamana (southern) sub-provinces. Sr–Nd isotope compositions display a trend from depleted ($\epsilon_{\text{Nd}} = +7.5$; $\text{Sr}_i = 0.7030$; Antsoha end-member) to highly enriched products ($\epsilon_{\text{Nd}} = -17$; $\text{Sr}_i = 0.7228$; Manamana end-member). Antsoha end-member is considered to be located at the lithosphere–asthenosphere boundary while the composition of Manamana end-member implies a location within the Archean to Proterozoic continental lithosphere. Oligocene Ankaratra HTP alkaline province, Miocene Ankilioaka transitional province, Pliocene Ambre Mountain and Pleistocene Nosy Be Island alkaline volcanoes display a restricted isotopic range ($\epsilon_{\text{Nd}} = +4$ to 0; $\text{Sr}_i = 0.7032$ to 0.7048) forming an array distinct from the Cretaceous trend, implying the enriched pole did not correspond to Manamana end-member. This Cenozoic array could result from mixing between Antsoha end-member and BSE or a pole beyond. The exceptional variation of mantle sources involved in the Cretaceous episode contrasts with the more homogeneous near-BSE source during the Cenozoic. Several lines of evidence dismiss the mantle plume model. Cretaceous volcanism resulted from reactivation of a lithospheric scale shear zone due to plate reorganisation that eventually led to the Madagascar–India continental break-up. The lower lithospheric/asthenospheric melt (Antsoha end-member) was able to melt the most enriched/fusible parts of an upper lithospheric mantle (Manamana end-member); these two melts partly mixed. Long-lasting Neogene volcanic activity was less voluminous. The melting source was restricted to a lower part of the lithospheric mantle.

© 2009 International Association for Gondwana Research. Published by Elsevier B.V. All rights reserved.

1. Introduction

The great variety of basaltic magmas outpouring at the surface of the earth has been linked to mantle compositions as well as to the different petrogenetic processes operating at different depth levels. Madagascar, one of the largest islands in the world, is composed of a continental fragment detached from Gondwana during the Mesozoic and has been the focus of several studies to unravel the history of amalgamation of the Gondwana supercontinent and related tectonic processes (Collins, 2006; Tucker et al., 2007; Rakotondrazafy et al.,

2007). It has been debated whether Madagascar is an island or a continent (de Wit, 2003). In addition, this crustal fragment represents a case of protracted volcanic processes from the Cretaceous to the present. During such a long period of time, it is expected that source rocks may change.

While basaltic magmas are generally thought to come from the mantle, their present compositions, especially their incompatible trace elements, suggest that they are not primary magmas, but were strongly differentiated through spinel + olivine fractionation. Basaltic compositions result from both the source compositions subjected to partial melting, and from the rate (extent and depth) of melting (for a review, see Bardintzeff et al., 1994 and references therein), as evidenced by the transition from tholeiitic to alkaline basic lavas in Hawaii (Macdonald and Katsura, 1964) and other volcanic islands such as those of French Polynesia. Mantle heterogeneities are evaluated through isotopes, e.g., the various end-members named HIMU, DMM, EM1 and EM2, PREMA, FOZO (Zindler and Hart, 1986;

* Corresponding author. Laboratoire de Pétrographie-Volcanologie, UMR CNRS IDES 8148, Bât. 504, Université Paris-Sud, 91405 Orsay Cédex, France. Tel.: +33 1 69 15 67 44; fax: +33 1 69 15 49 05.

E-mail addresses: jacques-marie.bardintzeff@u-psud.fr (J.-M. Bardintzeff), jean-paul.liegeois@afriamuseum.be (J.-P. Liégeois), bernard.bonin@u-psud.fr (B. Bonin), hervé.bellon@univ-brest.fr (H. Bellon).

White, 1995; Stracke et al., 2005; Zhu, 2007), as well as by trace elements (Weaver, 1991a,b).

The aim of this paper is to explore the source characteristics of the volcanic suites using trace element and isotopic evidence.

2. Geodynamic context and geological settings

The Gondwana supercontinent (see reviews in de Wit 1999; Storey et al., 2000a,b; Bumby and Guiraud, 2005; Meert and Lieberman, 2008; Rino et al., 2008; Santosh et al., 2009) broke up during the period lasting from Mid-Jurassic to Mid-Cretaceous (Rakotosolofa et al., 1999; Piqué et al., 1999). After approximately 100 Ma of crustal extension (Schandlmeier et al., 2004), Madagascar was first disconnected from the Kenya–Somalia part of the African continent, during the Middle to Upper Jurassic, by dextral transcurrent movement along the Davie Ridge within the Mozambique Channel (Coffin and Rabinowicz, 1987; Cox,

1988; Raillard, 1990; Kusky et al., 2007; Papini and Benvenuti, 2008; Fig. 1). This separation of Madagascar could have occurred since the Late Liassic according to Geiger et al. (2004). Later, during the Upper Cretaceous, a new dislocation took place between Greater India and Madagascar (Storey et al., 1995; Pande et al., 2001).

Madagascar witnessed several volcanic episodes after separation of Greater India (Besairie et al., 1957; Besairie, 1972; Fig. 1). The vast majority of the lavas were erupted during the Upper Cretaceous (Albian and Turonian), when Madagascar was ultimately separated from Greater India, and the flood basalts are likely to have covered the entire surface of the island. Remnants of the volcanic pile are preserved in the Mesozoic sedimentary basins of the western coast, namely the Morondava Basin (Rasamimanana, 1996; Gioan et al., 1996; Rasamimanana et al., 1998; Bardintzeff et al., 2001), the Mailaka Basin (Melluso et al., 2001), the Majunga Basin (Rasamimanana, 1996; Melluso et al., 1997, 2002, 2003), the southern coast with the Volcan de l'Androy (Mahoney et al., 1991; Dostal et al., 1992; Storey et al., 1995; Rasamimanana, 1996; Storey et al., 1997; Mahoney et al., 2008), and the eastern coast (Storey et al., 1995, 1997).

Volcanic activity was resumed during the Cenozoic. The volcanic products of Itasy and Ankaratra in the centre of the island were emitted during the Neogene. Minor products were emitted during the Miocene at Ankililoaka near the western coast (Rasamimanana, 1996; Rasamimanana et al., 1998), and near Lavanono in the south. Rather voluminous Pliocene–Quaternary products are exposed at the Ambre Mountain, north of Madagascar (Melluso et al., 2007), and in the island of Nosy Be (Karche, 1973; Nougier et al., 1986; Rasamimanana, 1996; Melluso and Morra, 2000), that are classically related to the Seychelles–Comores hot spot.

Numerous intrusions, which appear to be approximately of the same age as the volcanic rocks (Cretaceous), outcrop on the island of Madagascar, essentially along the western and eastern coasts. One of them, the Antampombato–Ambatovy Complex has been studied in detail by Melluso et al. (2005).

This paper focuses on four volcanic provinces of Madagascar, the Cretaceous Morondava flood–basalt sequence, the Cenozoic Ankaratra suite, the Miocene Ankililoaka province, and the Pliocene–Quaternary assemblage of Ambre Mountain and Nosy Be Island, with emphasis on their trace element contents and Sr–Nd isotopic signatures. We compare the data with those of other provinces of Madagascar and the Marion Island formations.

3. K–Ar chronology

32 new K–Ar Cretaceous and Neogene ages are listed in Table 1.

K–Ar dating was performed on whole-rock lava samples. Most of the selected samples are fresh in terms of their wt.% LOI of less than 2%, except five samples (C85, C7, C104, C111, C146) with LOI ranging from 2 to nearly 4 wt.%, probably linked to late hydrothermal processes. Lavas contain fresh plagioclase crystals and in some cases up to 15 vol.% secondary minerals. The only exception is lava C82 which contains up to 40 vol.% of secondary minerals. However, the groundmasses of some lavas have been altered to differing degrees. A peculiar attention has been carried for low-K lavas.

After crushing and sieving, the 0.3 to 0.15 mm size fraction was cleaned with distilled water. This fraction was retained for two analytical purposes: (a) one aliquot for K analysis by atomic absorption after hydrofluoric solution of the powder ground in an agate grinder, (b) a second aliquot was used for argon extraction and further isotopic analyses. Argon was extracted under high vacuum by induction heating of a molybdenum crucible. Extracted gases were cleaned in three successive titanium sponge furnaces and ultra-purified by using one Al–Zr SAES getter. Isotopic composition of argon and concentration of radiogenic ^{40}Ar were measured using a 180° -geometry stainless steel mass spectrometer equipped with a 642 Keithley amplifier. Isotopic dilution was realised with a ^{38}Ar spike buried as ions in Al targets following the procedure described by

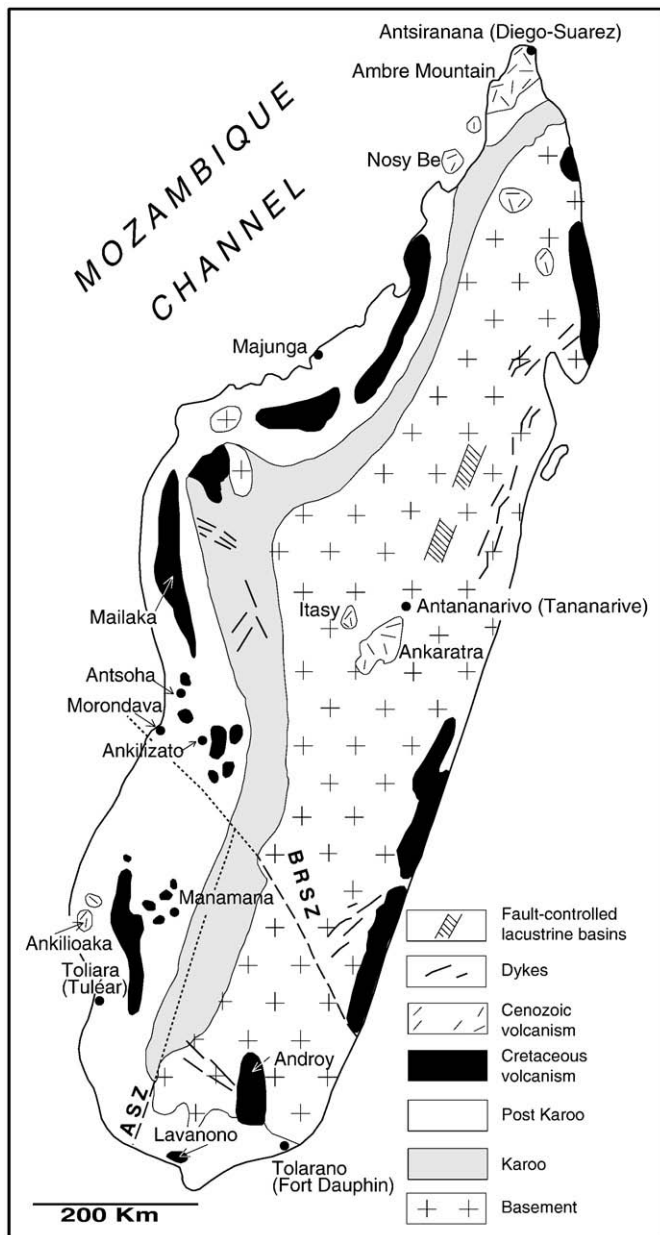


Fig. 1. Volcanic units of Madagascar (modified after Rasamimanana et al., 1998) and major shear zones (after Shackleton, 1996). Dashed line: exposed shear zone, dotted: inferred, unexposed shear zone. ASZ=Ampanihy shear zone, BRSZ=Bongolava–Ranotsara shear zone.

Table 1

K–Ar isotopic data on Cretaceous (Morondava, Majunga, Androy) and Tertiary and Quaternary rocks (Ankaratra, Ankilioaka, Ambre Mountain, Nosy Be Island) volcanic rocks. Constant values of Steiger and Jäger (1977) were used and uncertainties have been calculated using equations of Mahood and Drake (1982). Analytical procedures are described in the text.

Sample	Rock type*	Analysis number	Age ± error (Ma)	Average (Ma)	K ₂ O (wt.%)	LOI (wt.%)	⁴⁰ Ar _R (%)	⁴⁰ Ar _R 10 ⁻⁷ cm ³ /g	Weight (g)
<i>Morondava</i>									
C'11	HTP olivine basalt	B3998	86.2 ± 2.0	87.7 ± 2.1	0.97	1.13	81.8	27.62	0.5079
		B3927	89.1 ± 2.1				75.1	28.55	0.5138
C'4	HTP olivine basalt	B3926	79.9 ± 1.9		1.15	1.09	76.2	30.31	0.5059
C85	HTP ferrobasalt	B4004	64.9 ± 1.5		0.60	2.42	82.2	12.79	0.7052
C86	HTP ferrobasalt	B4174	64.5 ± 1.5		0.78	1.26	72.3	16.52	0.6018
C162	HTP basalt	B3995	69.5 ± 1.6		1.16	0.48	90.9	26.49	0.7045
C79	HTP andesitic basalt	B3992	58.5 ± 1.4	60.7 ± 1.5	1.09	0.83	84.8	20.91	0.7048
		B4001	62.9 ± 1.5				79.9	22.50	0.7011
C82	HTP andesitic basalt	B4005	39.3 ± 0.9	40.6 ± 1	1.35	0.98	81.0	17.29	0.7009
		B3993	42.0 ± 1.0				80.0	18.48	0.7013
C71	LTP andesitic basalt	B3934	93.5 ± 2.2		0.88	1.63	66.5	27.24	0.5028
C20	LTP basalt	B4000	87.9 ± 2.1		0.34	0.68	74.7	9.88	0.8009
C22	LTP basalt	B3990	83.3 ± 1.9		0.35	1.57	78.7	9.61	0.7110
C9	LTP basalt	B3989	80.4 ± 1.9		0.39	1.05	74.1	10.33	0.7049
C73	LTP andesitic basalt	B3996	61.6 ± 1.4		1.10	0.94	87.1	22.20	0.7049
C14	Dolerite	B3997	89.6 ± 2.1		1.86	1.47	89.8	55.08	0.5015
C7	Gabbro	B4368	79.7 ± 2.9	79.3 ± 9	0.185	3.57	30.3	4.85	0.6033
		B4003	78.9 ± 2.1				51.4	4.81	0.6082
<i>Majunga</i>									
C70	Dolerite	B3928	91.2 ± 2.3		0.17	1.23	50.9	5.12	0.8138
C67	Basalt	B3935	65.6 ± 1.5		0.74	0.98	70.5	15.93	0.6087
C64	Basalt	B4175	65.4 ± 1.5		0.72	1.12	72.1	15.46	0.6308
<i>Androy</i>									
C146	Upper basalt	B3973	103.0 ± 2.4	103.4 ± 2.5	0.87	2.93	71.6	29.75	0.8014
		B4369	103.8 ± 2.5				66.9	29.96	0.6040
C152	Lower basalt	B3988	86.0 ± 2.0		1.19	1.36	97.3	33.79	0.8070
C144	Upper basalt	B3954	83.2 ± 2.0		1.49	1.83	49.4	40.93	0.5326
C149	Upper rhyolite	B3958	78.2 ± 1.8		4.75	1.51	90.8	122.40	0.3040
<i>Ankaratra</i>									
Ank3	HTP basalt	B4438	27.9 ± 0.7	27.9 ± 0.7	1.36	1.77	68	12.3	0.8021
		B4460	27.9 ± 0.7				55.6	12.34	0.7312
Ank5	HTP basalt	B4440	17.2 ± 0.4		1.25	0.60	65	6.966	0.8034
Ank1	HTP basalt	B4434	17.2 ± 0.4		2.08	1.74	59.7	11.6	0.8039
Ank2	HTP basalt	B4435	17.7 ± 0.4		1.52	0.98	58.5	8.702	0.6121
Ank4	HTP basalt	B4439	11.4 ± 0.6	11.4 ± 0.6	1.07	1.92	36.9	3.957	0.8006
		B4461	11.3 ± 0.4				30.9	3.905	0.7060
Ank6	HTP basalt	B4453	3.36 ± 0.12	3.11 ± 12	1.54	0.32	25.7	1.67	0.8040
		B4463	2.86 ± 0.11				24.5	1.419	0.7473
<i>Ankilioaka</i>									
C90	LT/HP andesitic basalt	B4002	9.37 ± 0.29		1.49	0.94	31.7	4.511	0.5029
C87	LTHP basalt	B3994	8.95 ± 0.24		1.01	1.11	36.4	2.923	0.7173
<i>Ambre Mountain</i>									
C104	Basanite	B3953	1.88 ± 0.13		1.46	2.53	11.8	0.884	0.7001
<i>Nosy Be Island</i>									
C111	HTP basanite	B5986	1.64 ± 0.07		1.3	3.87	20.5	0.688	1.0125
C107	HTP basanite	B3987	0.55 ± 0.04		1.61	0.08	11.2	0.285	1.0082

* Rock types are named according to Bardintzeff et al. (2001), see text.

Bellon et al. (1981). ³⁸Ar contents were regularly checked using the GLO-glaucinite international standard (Odin and Hunziker, 1982).

Ages have been calculated using the constants recommended by Steiger and Jäger (1977). Errors in age at ± 1 σ level have been quoted following the equation by Mahood and Drake (1982).

Fig. 2 presents modal percentages of secondary minerals vs. isotopic ages. It evidences a difference between magmatic ages (between 93 and 79 Ma) with less than 10% of secondary minerals and rejuvenated ages (between 70 and 39 Ma, intermediate between ages of emplacement of rocks and ages of secondary parageneses) with more than 2% and up to 40% of secondary minerals.

The Cretaceous Morondava province is located in western Madagascar. 14 whole-rock K–Ar age determination (in Rasamimanana et al., 1998; Table 1) cluster into two groups: (a) 8 mostly

porphyritic lavas, with less than 3 vol.% of secondary minerals (Fig. 2) yielded results ranging between 93.5 ± 2.2 Ma and 78.9 ± 2.1 Ma, (b) 5 aphyric samples containing from 5 to 15 vol.% of secondary minerals have ages ranging from 69.5 ± 1.6 Ma to 61.6 ± 1.4 Ma. An exceptionally young age of 41 ± 1 Ma was found in the aphyric lava C82. This rock contains up to 40 vol.% of secondary minerals; its abundant groundmass is strongly chloritised.

We interpret the oldest age (93 Ma corresponding to the Turonian) of the first group as dating the magma outpouring of flood basalts. The Turonian igneous event was also active along the eastern coast of the island as evidenced by the plateau ⁴⁰Ar–³⁹Ar ages obtained for separated plagioclases (Storey et al., 1995).

This group comprises the C20, C22, C9 low-K (less than 0.5 wt.% K₂O) basalts as well as mildly K-rich (more than 0.6 wt.% up to 1.3 wt.% K₂O)

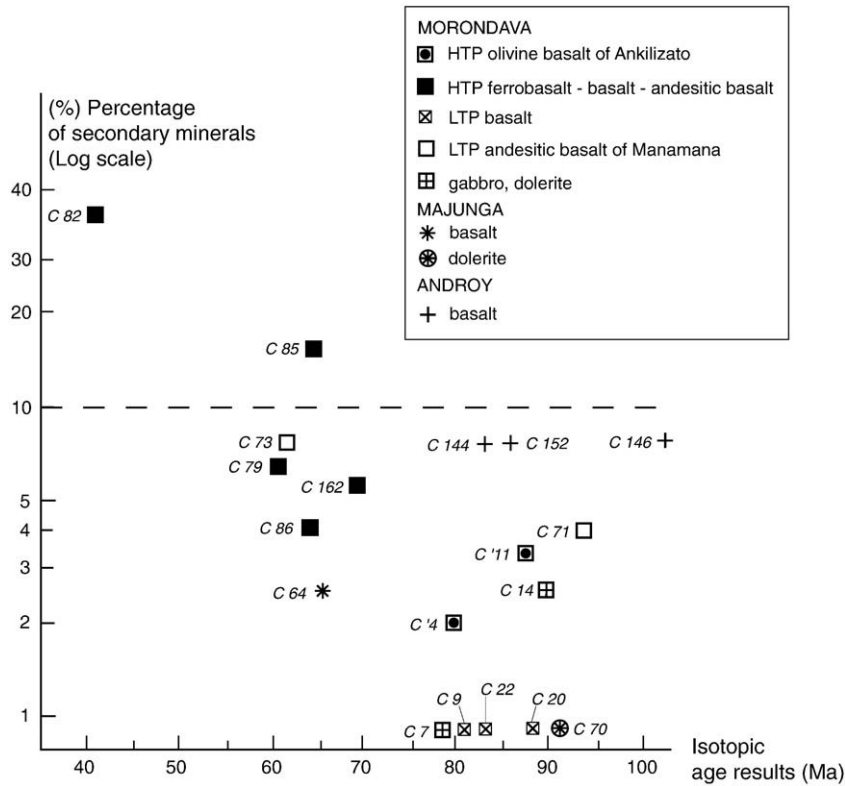


Fig. 2. Percentage of secondary minerals in dated rocks.

basalts. It is important to note that the dates obtained are not a function of K₂O contents. The apparent age range is basically due to incipient alteration.

The second group of younger ages is related to rejuvenation effects promoted by a persistently high thermal regime and/or late hydrothermal alteration during Late Cretaceous and even Paleogene, as evidence by the correlation of dates with LOI.

New age determinations for Majunga and Androy volcanic activity are also listed in Table 1. Though less numerous than for Morondava, these results show a similar range. For Majunga, one age is 91.2 Ma (low-K fresh dolerite C70 with 0.17 wt.% K₂O) and two others yield ca. 65 Ma ages for lavas with partially devitrified and replaced groundmass. For Androy, three ages (86 to 78 Ma) are in good agreement with the stratigraphical succession from the lower basalt to the upper rhyolite. The anomalously old age obtained for lava C146 denotes probable leaching of K correlated with higher LOI (2.93 wt.%). Likely igneous ages are in the same range as those obtained by Storey et al. (1995) and Mahoney et al. (2008).

The Cenozoic Ankaratra province occupies the Central Madagascar region. 6 whole-rock K–Ar age determinations (Table 1), ranging from 28 to 3 Ma, seem to indicate four discrete volcanic episodes between Oligocene and Pliocene, respectively at ca. 28 Ma, Chattian (one sample), ca. 17 Ma, Burdigalian (three samples), ca. 11.5 Ma, Serravallian (one sample); and ca. 3 Ma, Piacenzian (one sample).

The Ankilioaka province, West Madagascar, was emplaced in the southern part of Morondava Basin, in Upper Miocene (Tortonian) time as shown by whole-rock K–Ar ages of 9.4 to 8.9 Ma (Rasamimanana, 1996; Rasamimanana et al., 1998; Table 1).

Lastly, the Ambre Mountain and Nosy Be Island volcanoes, North Madagascar, are dated at 1.88–0.55 Ma, Pliocene–Pleistocene (Rasamimanana, 1996; Rasamimanana et al., 1998; Table 1). Emerick and Duncan (1982) reported older ages of 9.4 to 9.1 Ma for Cap d’Ambre, 10.15 ± 0.73 Ma for Nosy Komba SE of Nosy Be, and 7.32 ± 0.26 Ma for Befotaka in Nosy Be.

The Neogene volcanic activity appears to represent discrete events rather than a more or less continuous episode.

Table 2 Summary of the petrological and mineralogical characteristics of the volcanic rocks of different provinces of Madagascar.

Province	Number of analyses	Rock nomenclature (Le Maitre, 2002)	Rock specific name	Phenocrysts	Microliths	SiO ₂ (wt.%)	Qz or Ne (wt.%) CIPW norm	Affinity	HTP/LTP
Morondava									
Centre	3	Basalt	Olivine basalt	ol, (mt)	pl, mt, ol, cpx	45.2–46.7	2.8–4.3 Ne	Alkaline	HTP
South	4	Basalt	Ferrobasalt	–	pl, cpx, ilm	47.6–48.3	1.1–3.0 Qz	Tholeiitic	HTP
South	9	Basalt	Basalt	–	ilm, cpx, pl	49.3–51.2	3.5–8.4 Qz	Tholeiitic	HTP
South	5	Basaltic andesite	Andesitic basalt	(pl), (cpx)	cpx, pl, (ilm)	51.8–53.9	5.0–9.2 Qz	Tholeiitic	HTP
Centre	13	Basalt	Basalt	cpx, (ol), (mt)	pl, cpx, mt, (ol)	46.7–48.6	0.0–8.5 Ne	Alkaline	LTP
South	6	Basalt + basaltic andesite	Andesitic basalt	(pl), (cpx), (mt)	pl, cpx, mt	50.4–52.9	0.0–4.3 Qz	Tholeiitic	LTP
Ankaratra	6	Basalt + trachybasalt	–	pl, cpx, (ol)	pl, mt, (ol), (cpx)	44.9–49.5	0.2–6.5 Ne	Alkaline	HTP
Ankilioaka	4	Basalt	–	ol, cpx, pl	pl, cpx, mt	50.5–52.0	0.0–0.9 Qz	Transitional	LT/HP
Ambre Mt.	9	Basanite	–	ol	ol, pl, cpx, mt, (ilm)	42.0–44.9	0.0–14.1 Ne	Alkaline	HTP
	11	Basalt	–	ol	ol, pl, cpx, mt	45.2–50.4	0.0–4.5 Ne	Alkaline	LTP
Nosy Be	3	Basanite	–	ol, amp	ol, pl, cpx, mt, (ilm)	42.9–44.0	14.4–14.6 Ne	Alkaline	HTP

4. Petrology, major and minor elements

The main petrological and mineralogical characteristics of samples analysed are listed in Table 2.

Samples were analysed at Brest and Orsay, using inductively coupled plasma atomic-emission spectrometry (ICP-AES), except Rb which was measured by flame-emission spectroscopy. Samples were powdered in an agate grinder. Major and trace elements were analysed without chemical separation (Cotten et al., 1995). International standards (ACE, BEN, JB-2, PMS and WSE) were used for calibration tests. Relative standard deviations were ca. 1% for SiO₂ and 2% for other major elements, except for P₂O₅ and MnO concentrations at ±0.01%, and ca. 5% for trace elements.

Almost all the lavas studied contain plagioclase, clinopyroxene and Fe–Ti oxides, occasional olivine and scarce amphibole, in various proportions, as phenocrysts as well as microcrysts within the groundmass. They have mafic to intermediate chemical compositions (42 to 54 wt.% SiO₂), and contain CIPW-normative quartz or nepheline.

According to the TAS nomenclature scheme (Le Maitre, 2002), the suite includes mostly basalts, some basanites, less common basaltic andesites, and rare trachybasalts (hawaiites). In the case of Morondava Basin, they occupy overlapping fields in the TAS diagram, and the different suites were given more specific names, i.e. olivine basalt, ferrobasalt, and andesitic basalt (Bardintzeff et al., 2001).

As far as Ti and P are concerned, two contrasting populations are present in the Morondava Basin (Bardintzeff et al., 2001): high-Ti–P (TiO₂ > 2 wt.%, P₂O₅ > 0.4 wt.%) and low-Ti–P (TiO₂ < 2 wt.%, P₂O₅ < 0.4 wt.%) (Tables 2 and 3, Fig. 3). These will be referred to hereafter as HTP and LTP, respectively. Ti and P behave in a similar manner (Fig. 3b and d), suggesting a control by Ti-bearing oxides, most probably rutile, and an additional P-bearing phase, most probably apatite. Both HTP and LTP groups are found elsewhere in Madagascar: the southernmost region (Dostal et al., 1992), the northern region (Melluso et al., 1997), and along the eastern coast (Storey et al., 1997). The association of two coeval HTP and LTP suites is well known in CFB provinces throughout the Gondwana supercontinent, e.g., the Karoo basalts of South Africa–Lesotho, the Deccan traps of Greater India, and the Paraná–Etendeka province of Brazil–Namibia (Hawkesworth et al., 1999).

4.1. Volcanic formations of the Morondava Basin

Along 700 km of the western coast, in the region of Morondava Basin, a thick blanket of basaltic rocks, typical of Continental Flood Basalts (CFB), is exposed in various places. The Morondava Basin rests upon two discrete Precambrian, central and southern, terranes separated by the Bongolava–Ranotsara shear zone. Rocks from the central (in the vicinity of Ankilizato, Fig. 1) and southern (near Manamana) areas have been sampled.

Silica saturation is highly variable, with CIPW-normative compositions ranging from 8.5% nepheline to 9.2% quartz (Tables 2 and 3). The Differentiation Index (DI = wt.% CIPW-normative quartz + orthoclase + albite + nepheline) increases steadily from 22.1 to 39.1. The high-Ti–P (HTP) family includes four volcanic rock types, labelled as: olivine basalt, ferrobasalt, basalt sensu stricto and andesitic basalt. In this family, the more mafic, more alkaline porphyritic olivine basalt yields CIPW-normative nepheline and constitutes a specific group. The almost aphanitic suite of ferrobasalt, basalt s.s. and andesitic basalt defines a silica-oversaturated tholeiitic series, with a continuous liquid line of descent from Fe- and Ti-rich mafic towards more silica-rich compositions.

The low-Ti–P (LTP) family includes only two volcanic rock types: basalt s.s. and andesitic basalt. Though the term “andesitic basalt” is not used in the TAS diagram (Le Maitre, 2002), we use it herein to describe compositions that straddle the basalt–basaltic andesite boundary. The porphyritic LTP family is highly heterogeneous. Basalt

s.s. has alkaline affinities marked by relatively Na-rich compositions, while the andesitic basalt is tholeiitic and relatively poorer in Na.

The Morondava Basin is occupied by two discrete magmatic provinces (Fig. 3): (a) the southern province is dominantly tholeiitic, with CIPW-normative quartz, and comprises the HTP ferrobasalt–basalt–andesitic basalt series and the LTP andesitic basalt group of Manamana, and (b) the central province has alkaline affinities and is characterised by the CIPW-normative nepheline LTP basalts of Antsoha and HTP olivine basalts of Ankilizato.

Bulk-rock major element compositions show large variations in the lavas of Morondava but MgO contents are of the same order of magnitude in the different suites (Table 4). Their compositional differences, therefore, cannot be related to various degrees of partial melting of the same source. More likely, they represent the combination of multiple sources (e.g. Bardintzeff et al., 1994) and/or various extents of crustal contamination (e.g. Dostal et al., 1992). Regardless of their CIPW-normative compositions, all the igneous rocks have #mg ranging between 57 and 36.5.

4.2. The Ankaratra province

Ankaratra is an alkaline volcanic province in Central Madagascar, well known as the type-locality for “ankaratrite”, a melanocratic variety of biotite-bearing olivine nephelinite (Lacroix, 1916). The samples used herein are typical HTP basalts and trachybasalts (Tables 2–4), with olivine, clinopyroxene and plagioclase phenocrysts, CIPW-normative nepheline reaching up to 6.5 wt.%. No ankaratrite sensu stricto has been sampled.

4.3. The Ankilioaka area

In the southern part of the Morondava Basin, near Ankilioaka, north of the town of Tuléar, the Cenozoic sedimentary formations are crosscut by dykes and overlain by lava flows. This renewed Miocene volcanic activity seems to be related to movements along the Tuléar fault zone. The lavas are basalts, marked by distinctive medium-Ti (1.8–2 wt.% TiO₂) and high-P (0.45–0.57 wt.% P₂O₅). Their porphyritic texture comprises plagioclase phenocrysts (0.5-mm in size) as the major phase, with minor olivine and clinopyroxene phenocrysts (up to 2-mm). The groundmass is composed of plagioclase, clinopyroxene and magnetite microcrysts (Table 2).

The Ankilioaka rocks (Table 3) have slightly evolved compositions in terms of DI (30.6–37.8) which suggest low rates of partial melting. They have transitional, instead of tholeiitic, affinities with a range from 8.4 wt.% CIPW-normative olivine to 0.9 wt.% CIPW-normative quartz.

4.4. Nosy Be Island and Ambre Mountain recent volcanoes

Nosy Be Island and Ambre Mountain, Northern Madagascar, display Pliocene–Pleistocene volcanoes.

In Nosy Be, basanite is characterised by high TiO₂ (2.3–2.7 wt.%) and P₂O₅ (0.5–0.8 wt.%) contents. Melluso and Morra (2000) have described tephrite and phonotephrite as well.

The Ambre Mountain formations comprise two distinct suites: the HTP basanite, identical to Nosy Be, is associated with phonolite (Rasamimanana, 1996), while the LTP basalt resembles the LTP alkali basalt of Morondava in terms of TiO₂ (1.5–1.8 wt.%) and P₂O₅ (0.2–0.4 wt.%) contents (Tables 2 and 3).

5. Trace and rare earth elements

5.1. Volcanic formations of the Morondava Basin

All the rocks have low Cr and Ni contents (less than 150 ppm and 72 ppm, respectively). These values are much lower than those

Table 3
Selected chemical analyses and CIPW norms (calculated with 1.5 wt.% Fe₂O₃) of representative lavas. LOI for Loss On Ignition. DI (Differentiation Index) is the sum of CIPW-normative (Qz + Or + Ab + Ne). Analyses by J. Cotten, UBO Brest, except C82, C45 and C97 by R. Coquet, UPS Orsay.

Age (Ma)	Morondava						Ankaratra						Ankiloaoka	Ambre Mt.		Nosy Be	
	High-Ti-P			Low-Ti-P			High-Ti-P						Low-Ti-HP	HighTiP	LowTiP	HighTiP	
	Olivine basalts		Ferrobas.	Basalt	And. bas.	Basalts	And. bas.	Basalts						And. bas.	Basanite	Basalt	Basanite
	Centre - Ankilizato		South	South	South	Centre - Antsoha	South - Manamana										
	C'11	C'4	C85	C91	C82	C'20	C3	C71	C73	Ank3	Ank5	Ank4	Ank6	C90	C45	C97	C107
	87.7	79.9	64.9		41			93.5	61.6	27.9	17.2	11.4	3.10	9.37			0.55
<i>wt.%</i>																	
SiO ₂	46.50	46.70	47.60	49.70	51.81	47.80	47.90	50.50	51.90	46.15	45.80	45.70	44.90	52.00	42.97	46.53	43.80
TiO ₂	2.42	2.45	3.43	3.13	3.04	1.49	1.72	1.19	1.37	2.29	2.91	2.39	2.32	2.00	2.30	1.56	2.41
Al ₂ O ₃	16.70	16.80	13.40	13.45	13.64	17.35	17.05	14.15	13.70	13.90	15.17	13.13	13.80	13.95	13.93	13.18	13.62
Fe ₂ O ₃	12.35	12.50	15.30	14.85	13.86	12.04	12.50	12.50	13.45	12.35	13.04	11.77	12.38	10.62	12.67	12.90	12.10
MnO	0.20	0.20	0.18	0.18	0.21	0.19	0.19	0.18	0.21	0.16	0.17	0.17	0.19	0.20	0.20	0.18	0.19
MgO	6.83	6.43	4.95	4.68	4.38	4.64	4.65	6.31	4.99	6.50	6.95	8.84	9.32	5.49	9.85	12.90	10.66
CaO	8.35	8.00	8.86	8.50	8.32	11.50	11.40	10.55	9.15	10.65	9.15	10.60	11.56	9.15	11.18	10.19	11.45
Na ₂ O	3.84	4.10	2.33	2.51	2.45	3.07	2.80	2.29	2.44	3.55	3.14	3.05	2.59	3.40	4.12	2.42	3.40
K ₂ O	0.97	1.16	0.60	0.83	1.29	0.39	0.34	0.82	1.03	1.34	1.26	1.00	1.58	1.37	1.02	0.72	1.68
P ₂ O ₅	0.54	0.55	0.46	0.42	0.38	0.21	0.20	0.14	0.17	0.87	1.20	0.90	0.72	0.57	0.67	0.30	0.57
LOI	1.13	1.09	2.42	1.14	1.05	0.92	1.81	1.63	0.94	1.77	0.60	1.92	0.32	0.94	1.08	-0.42	0.08
Total	99.83	99.98	99.53	99.39	100.43	99.60	100.60	100.26	99.35	99.53	99.39	99.47	99.68	99.69	99.99	100.46	99.96
#mg	52.52	50.72	39.29	38.66	38.73	43.53	42.68	50.24	42.59	51.28	51.60	60.03	60.09	50.83	60.86	66.67	63.79
<i>CIPW norm (wt.%)</i>																	
Qz			3.01	4.32	6.38			1.09	4.26					0.91			
Or	5.73	6.85	3.54	4.90	7.62	2.30	2.01	4.84	6.08	7.92	7.45	5.91	9.33	8.10	6.02	4.25	9.92
Ab	26.86	26.78	19.72	21.24	20.73	25.96	23.68	19.37	20.64	19.91	26.24	20.67	9.96	28.78	5.07	17.02	2.16
An	25.48	24.02	24.35	23.00	22.43	32.41	32.96	25.92	23.40	18.05	23.61	19.20	21.37	18.78	16.51	22.97	16.94
Ne	3.05	4.28								5.48	0.18	2.78	6.47		16.13	1.86	14.40
Di	10.19	9.93	13.88	13.75	13.69	19.37	18.58	21.10	17.46	23.95	11.47	22.36	25.44	18.83	28.11	20.72	29.24
Hy			21.35	20.49	18.35	1.20	8.31	20.30	20.05					15.06			
Ol	18.19	17.72				10.75	6.07			12.76	18.17	16.74	17.37		17.77	26.97	17.99
Mt	2.18	2.18	2.18	2.18	2.18	2.18	2.18	2.18	2.18	2.18	2.18	2.18	2.18	2.18	2.18	2.18	2.18
Il	4.61	4.66	6.53	5.96	5.79	2.84	3.27	2.27	2.61	4.36	5.54	4.55	4.42	3.81	4.38	2.97	4.59
Ap	1.19	1.21	1.01	0.92	0.84	0.46	0.44	0.31	0.37	1.91	2.64	1.98	1.58	1.25	1.47	0.66	1.25
DI	35.63	37.91	26.27	30.46	34.73	28.26	25.69	25.30	30.99	33.31	33.87	29.36	25.76	37.78	27.22	23.13	26.48
<i>ppm</i>																	
Rb	17.2	22.4	21	30	47.5	8.8	6.8	22	46	29	26	36	34	34.6	54.0	19.8	51
Sr	565	468	410	394	380	271	250	225	247	925	1273	1124	930	692	877	352	720
Ba	295	254	268	305	342	97	77	208	295	834	650	960	860	850	760	245	645
Sc	22	22	25	25		31	33	30	29	19.5	17.8	20	28	19.5			27
V	246	245	360	350	344	332	344	320	335	188	204	206	278	160	221	212	235
Cr	25	24	41	53	32.5	45	48	27	8	200	145	287	37.5	215	311	633	420
Co	38	37	51	47	41.9	42	42	50	50	45	41	44	47	52	51.0	64.3	54
Ni	45	43	40	36	26.9	49	41	57	31	150	83	187	163	79	214	372	230
Y	22.5	23	33	33	35.9	22	23	23.5	29.5	29	27.5	28	27.5	40	30.8	18.6	25
Zr	114	114	230	230	254	90	95	106	150	225	160	182	183	185	225	104	165
Nb	12.8	13	16.5	15.6	15.0	7.5	8.6	5	7.1	56.5	42	67	63	39.5	86.5	26.8	62
La	11.3	11.9	26.3	28	31.1	6.8	7.9	15.1	22.2	53	44.5	62.5	52	61.5	67.0	20.9	53
Ce	26	28	60	64	66.8	16.5	18	30.5	46	99	92	115	95	102	119	41.3	94
Nd	17.5	18	35.5	36.5	35.7	11.3	12	17.5	24	46.5	50	50.5	45	48.5	48.7	19.1	41.5
Sm	5	5.1	8.4	8.3	8.41	2.8	3.5	3.8	5.1	9.05	10	9.65	8.35	9.2	9.05	4.25	7.8
Eu	1.44	1.51	2.46	2.28	2.40	1.15	1.2	1.21	1.4	2.7	3.43	2.9	2.45	2.75	2.76	1.42	2.28
Dy	4.15	4.5	6.5	6.3	6.19	4	4.2	4.4	5.2	5.7	5.5	5.5	5.1	6.8	6.02	3.49	5
Er	2.2	2.2	3.4	3.3	3.24	2.3	2.3	2.5	3.1	2.55	2.4	2.35	2.6	3.5	2.77	1.85	2.4
Yb	2.01	2.05	2.67	2.6	2.75	2.04	2.15	2.21	2.6	2.07	1.73	1.93	2.03	2.4	2.50	1.46	2.02
Th	1.55	1.75	4.4	5.7	7.18	0.8	0.85	3.5	6	6.3	3.35	5.1	5.1	7.4	10.7	2.96	5.9

usually accepted for primary mantle magmas (see e.g., the normalising values of 250 ppm and 90 ppm, respectively, suggested by Pearce (1983) for MORB, liquids that are already differentiated), and provide strong evidence for extensive, multiply saturated fractionation of olivine + plagioclase ± clinopyroxene ± Fe-Ti oxides prior to the final eruption.

Nb abundances have a positive correlation with Ti but are not correlated with #mg or SiO₂, suggesting that magma compositions were controlled by one single Nb-Ti-bearing phase (possibly rutile). The uniformly high incompatible element contents point to variously enriched sources (Fig. 4). Primitive mantle-normalised values

(normalising values from Sun and McDonough, 1989) range from 10 to 70 for Rb and from 4.5 to 6 for Yb. The HTP and LTP families are clearly subdivided into four discrete suites, characterised by distinct LILE and HFSE patterns:

The olivine basalts of Ankilizato constitute a HTP group, where TiO₂ contents are only moderately high (about 2.5 wt.%), while P₂O₅ contents are very high (about 0.6 wt.%). Mantle-normalised spidergrams display a gently negative slope, with (Rb/Yb)_N = 8.5, and positive anomalies in K, Ba, Sr, P and Ti (Fig. 4a).

The HTP ferrobasalt-basalt-andesitic basalt series has more Ti (TiO₂ levels from 2.96 up to 3.47 wt.%), and less P (P₂O₅ levels

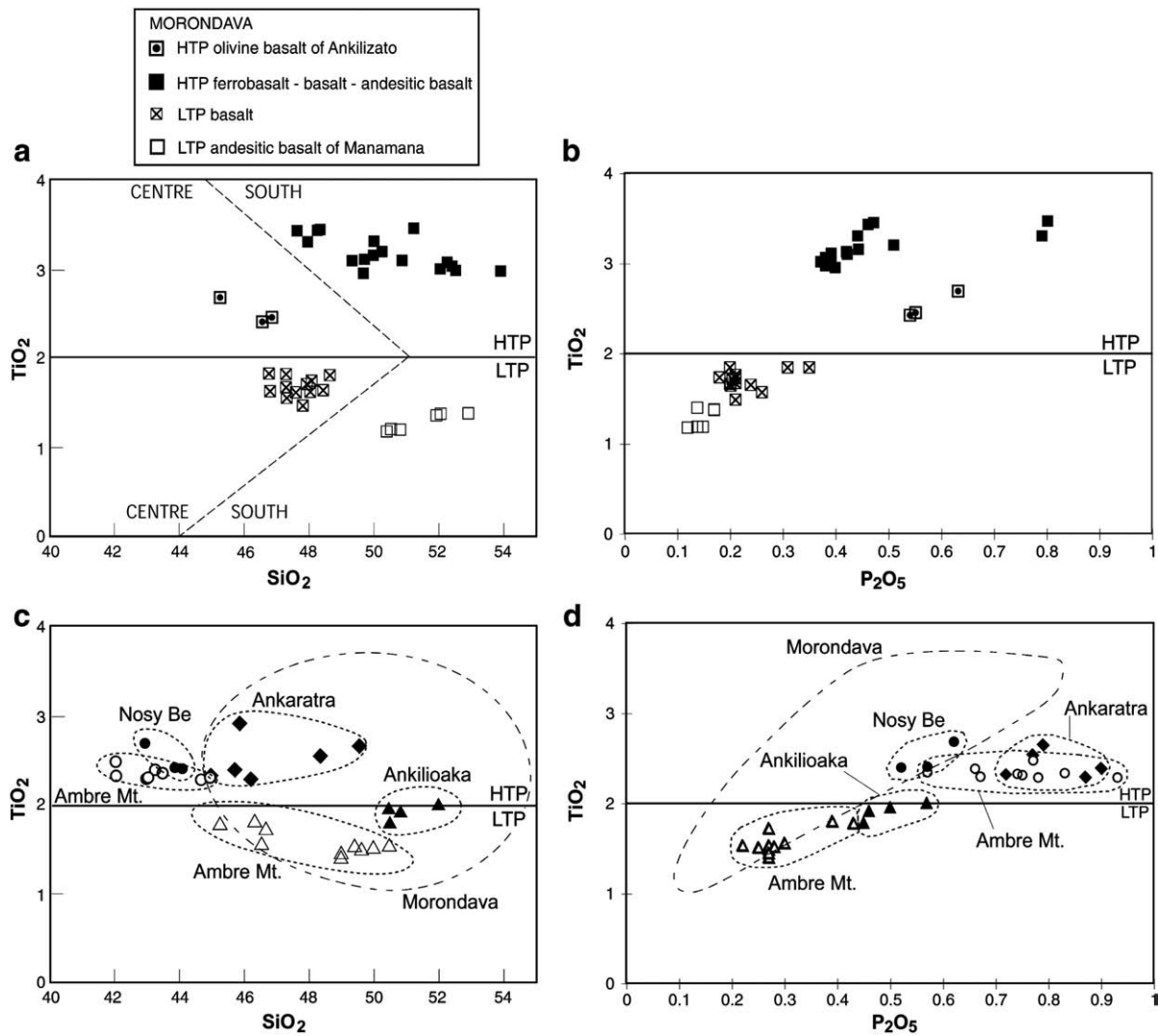


Fig. 3. (a) TiO₂/SiO₂ plot of the igneous formations of the Morondava Basin. Full line = HTP/LTP boundary, the dashed line indicates the boundary between the central and southern provinces. (b) TiO₂/P₂O₅ plot of the igneous formations of the Morondava Basin. (c) TiO₂/SiO₂ plot of different volcanic formations of Madagascar. Full line is the HTP/LTP boundary. The field of Morondava is delineated according to data of Fig. 3a. (d) TiO₂/P₂O₅ plot of different volcanic formations of Madagascar. The field of Morondava is delineated according to data of Fig. 3b.

between 0.37 and 0.51 wt.%, with two exceptions at 0.8 wt.%. Incompatible element contents are higher than in olivine basalts of Ankilizato. Mantle-normalised spidergrams display a gently negative slope, with $(Rb/Yb)_N = 8.0$, a clear positive anomaly in Th, negative anomalies in K, Nb and Sr and a less pronounced negative anomaly in P (Fig. 4b). Most anomalies are seen in the same elements as in the olivine basalts of Ankilizato, but with an opposite sign, i.e. positive vs. negative. LILE elements show more variations than HFS elements, maybe due to some late mobility.

The LTP basalts have quite different compositions. Incompatible element contents are considerably lower than the previous suites (TiO₂ contents in the 1.49–1.85 wt.% range, P₂O₅ contents in the 0.18–0.35 wt.% range). The normalised spidergrams have a rather flat pattern, with $(Rb/Yb)_N = 2.75$, which looks like E-MORB (Fig. 4c). They form three steps: 10 times the mantle values from Rb to Sr, with a slight positive anomaly in Sr and a negative anomaly in Th, 8 times the mantle values from Nd to Ti, with again a slight positive anomaly in Ti, and 5 times the mantle values for Y and Yb. C3 and C'20 samples are the more depleted in terms of Sr–Nd isotopes (see below). Their spidergrams could depict an asthenospheric mantle beneath Madagascar, especially that of C3 which presents nearly no anomalies in K

and Sr. In that way, C3-normalised spidergrams of all lavas have been also drawn for comparison (Fig. 5).

The LTP andesitic basalts of Manamana are very low in Ti (TiO₂ between 1.19 and 1.39 wt.%) and P (P₂O₅ between 0.12 and 0.17 wt. %). The mantle-normalised spidergrams are characterised by a sharp negative slope, with $(Rb/Yb)_N = 13$, deep negative anomalies in Nb and P, and less pronounced negative anomalies in Ba, Sr and Ti (Fig. 4d). From these patterns, coupled with the Sr–Nd isotopic data of Mahoney et al. (1991), Storey et al. (1997) argue that the LTP andesitic basalts of Manamana almost certainly assimilated continental crust.

5.2. The Ankaratra province

The HTP suite of Ankaratra is rich in LILE (up to 100 times the mantle value for Ba) and LREE (La at about 60–90 times the mantle values), but is poor in HREE (only 4 times the mantle value for Yb). Accordingly, mantle-normalised spidergrams (Fig. 4e) have a strong $(Rb/Yb)_N$ slope of about 14 and a higher $(Ba/Yb)_N$ slope of 34, with negative anomalies in Th, K, and Zr.

Table 4
Summary of the geochemical characteristics of the volcanic rocks of different provinces of Madagascar and comparison with end-members according to Melluso et al. (1997).

Province	Rock type	HTP/LTP	SiO ₂ wt.%	MgO wt.%	TiO ₂ wt.%	K ₂ O wt.%	Cr ppm	Ni ppm	Nb ppm	Sr ppm	Zr ppm	V ppm	Melluso et al.
Morondava	Olivine basalt	HTP	45.2–46.7	6.2–6.8	2.42–2.70	0.97–1.21	24–118	43–72	12.8–13.0	468–565	114–131	225–246	D1?
	Ferrobasalt	HTP	47.6–48.3	4.7–5.0	3.31–3.45	0.60–0.80	38–45	37–41	16.5–17.2	392–420	204–238	254–360	C
	Basalt	HTP	49.3–51.2	4.0–4.7	2.96–3.47	0.60–1.23	32–66	29–60	11.0–31.0	364–455	212–247	292–350	C
	Andesitic basalt	HTP	51.8–53.9	4.2–4.6	2.98–3.07	1.05–1.29	32–66	25–41	15.0–16.8	372–388	190–255	301–355	C
	Basalt	LTP	46.7–48.6	4.4–6.1	1.49–1.85	0.22–0.56	45–138	39–85	6.0–8.6	227–348	84–125	225–368	A
Andesitic basalt	LTP	50.4–52.9	5.0–6.3	1.18–1.39	0.40–1.11	8.0–31	31–60	5.0–7.3	217–247	94–151	314–345	A	
Ankaratra	Basalt + trachybasalt	HTP	44.9–49.5	3.8–9.3	2.29–2.91	1.00–2.11	4–287	3–187	42–67	852–1273	160–269	104–278	D? H Nb Sr
Ankilioaka	Basalt	LT/HP	50.5–52.0	5.5–7.3	1.78–2.00	0.59–1.37	215–341	79–199	30–39.5	520–692	143–185	152–180	
Ambre Mt.	Basanite	HTP	42.0–44.9	4.7–11.8	2.29–2.48	0.60–1.77	264–510	152–315	54–129	775–1003	172–315	187–235	D? H Nb Sr
	Basalt	LTP	45.2–50.4	8.1–12.9	1.40–1.80	0.40–1.06	287–648	200–372	17–42	287–467	90–140	194–223	A
Nosy Be	Basanite	HTP	42.9–44.0	9.4–10.7	2.40–2.69	0.71–1.68	352–430	190–244	62–83	720–744	165–196	235–250	D? H Nb Sr

5.3. The Ankilioaka area

High Ni and Cr contents (up to 199 ppm and 341 ppm, respectively) in the less silicic samples are close to primary magma compositions in equilibrium with the upper mantle. Nb contents are higher than in any other Upper Cretaceous formations of Morondava. Their primitive mantle-normalised spidergrams have LILE marked by a large negative anomaly in K and two positive anomalies in Ba and La. The chemical compositions of the LT/HP suite of Ankilioaka resemble so closely those of the HTP suite of Ankaratra that their mantle-normalised spidergrams (Fig. 4e) cannot be distinguished, suggesting their mantle sources and their evolutionary trends were identical.

5.4. Nosy Be Island and Ambre Mountain recent volcanoes

HTP basanite and LTP basalt families from both Nosy Be Island and Ambre Mountain display chemical features similar to the Ankilioaka and Ankaratra basalts: high MgO, Ni and Cr contents (Table 4) precluding extensive mineral fractionation and indicating compositions close to primary mantle-derived magmas. Trace element contents and behaviour are closely related to degrees of partial melting of the mantle source. The HTP suite of Ambre Mountain is approximately 2 to 3 times richer in all the incompatible elements than the LTP suite. The primitive mantle-normalised spidergrams (Fig. 4f) have smooth general shapes similar to those of Ankaratra and Ankilioaka suites, with a more pronounced negative anomaly in K. The large K trough can be attributed to the presence within the mantle source of K-bearing refractory minerals, such as phlogopite and/or K-rich amphibole.

6. Sr–Nd isotopic evidence

The new Rb–Sr and Sm–Nd isotopic results, obtained at the Isotope Geology division of the Royal Museum for Central Africa, Tervuren, Belgium, for different volcanic provinces of Madagascar, are listed in Table 5. Sr_i and ε_{Nd} values were calculated according to the known, or inferred, ages of emplacement.

After acid dissolution of the sample and Sr and/or Nd separation on ion-exchange resin, Sr isotopic compositions have been measured on Ta simple filament and Nd isotopic compositions on triple Ta–Re–Ta filament in a TIMS (thermal ionisation mass spectrometer) VG Sector 54. Repeated measurements of Sr and Nd standards have shown that between-run error is less than 0.000015 (2 σ). During the course of this study, the NBS987 standard yields values for ⁸⁷Sr/⁸⁶Sr between 0.710272 ± 0.000006 and 0.710278 ± 0.000009 (2 σ on the mean of the 4 standards measured for each set of 16 samples, normalised to ⁸⁶Sr/⁸⁸Sr = 0.1194) and the Rennes Nd standard values

for ¹⁴³Nd/¹⁴⁴Nd between 0.511962 ± 0.000008 and 0.511971 ± 0.000012 (2 σ on the mean of the 4 standards measured for each set of 16 samples, normalised to ¹⁴⁶Nd/¹⁴⁴Nd = 0.7219). All measured ratios have been normalised to the recommended values of 0.710250 for NBS987 and 0.511963 for Nd Rennes standard (corresponding to a La Jolla value of 0.511866). Blanks (around 0.1 ng) are negligible compared to the aliquots used during the geochemistry (2000 ng). The Rb–Sr and Sm–Nd ages have been calculated following Ludwig (2003). Decay constant for ⁸⁷Rb (1.42 × 10⁻¹¹ a⁻¹) was taken from Steiger and Jäger (1977) and for ¹⁴⁷Sm (6.54 × 10⁻¹² a⁻¹) from Lugmair and Marti (1978). Sr and Nd isotope ratios can be found in Table 5. Nd T_{DM} model ages were calculated following Nelson and DePaolo (1985).

For determining the mean age of the protolith of a geological unit, either magmatic or sedimentary, Nd T_{DM} model ages are a very powerful tool (DePaolo, 1983). The principle of the method is to calculate at what age the sample had the ¹⁴³Nd/¹⁴⁴Nd of the depleted mantle, thus approximating the mean age of its source. If the source is the depleted mantle alone, the Nd T_{DM} model age will be close to the actual age of the magmatic rocks. Generally, the rock is considered as coming from the mantle, i.e. is juvenile if the Nd T_{DM} model age = actual age + maximum 300 Ma, taking into account the variability of the Nd isotopic ratios in the mantle; if the source is multiple (i.e. a mantle source with a old continental contamination), the Nd T_{DM} model age will be intermediate between the two ages, closer to the contaminant source age when the contamination increases. Nd T_{DM} model ages give a maximum age for the intrusion and a minimum age for the oldest component of the source and a relative proportion when similar rocks are concerned. This calculation requires a realistic model for the depleted mantle; we prefer the evolution curve based on oceanic island arcs proposed by DePaolo (1981, 1983), for reasons discussed by Stern (2002). Nd T_{DM} model age calculations also assume that the ¹⁴⁷Sm/¹⁴⁴Nd of the rock remained constant since its generation (rare earth elements are difficult to mobilise except in melts) and this assumption is clearly valid here, as we are dealing with unmetamorphosed volcanic rocks. Finally, Nd T_{DM} model ages are valid only if the ¹⁴⁷Sm/¹⁴⁴Nd ratios of the rock is sufficiently different from the mantle ratio, for having sufficiently oblique evolution curves and hence a sufficiently well determined intersection; this is the reason why we limited the calculation of Nd T_{DM} model ages to samples having ¹⁴⁷Sm/¹⁴⁴Nd ratios < 0.165 following Stern (2002) (Table 5).

The effects of (hydro)thermal isotopic reset, though clearly affecting the K–Ar isotopic system, are less pronounced in the Rb–Sr system, because of low Rb/Sr ratios, as well as in the Sm–Nd system, because REEs are considered to be less prone to hydrothermal remobilisation. Thus, the Sr_i and ε_{Nd} values calculated

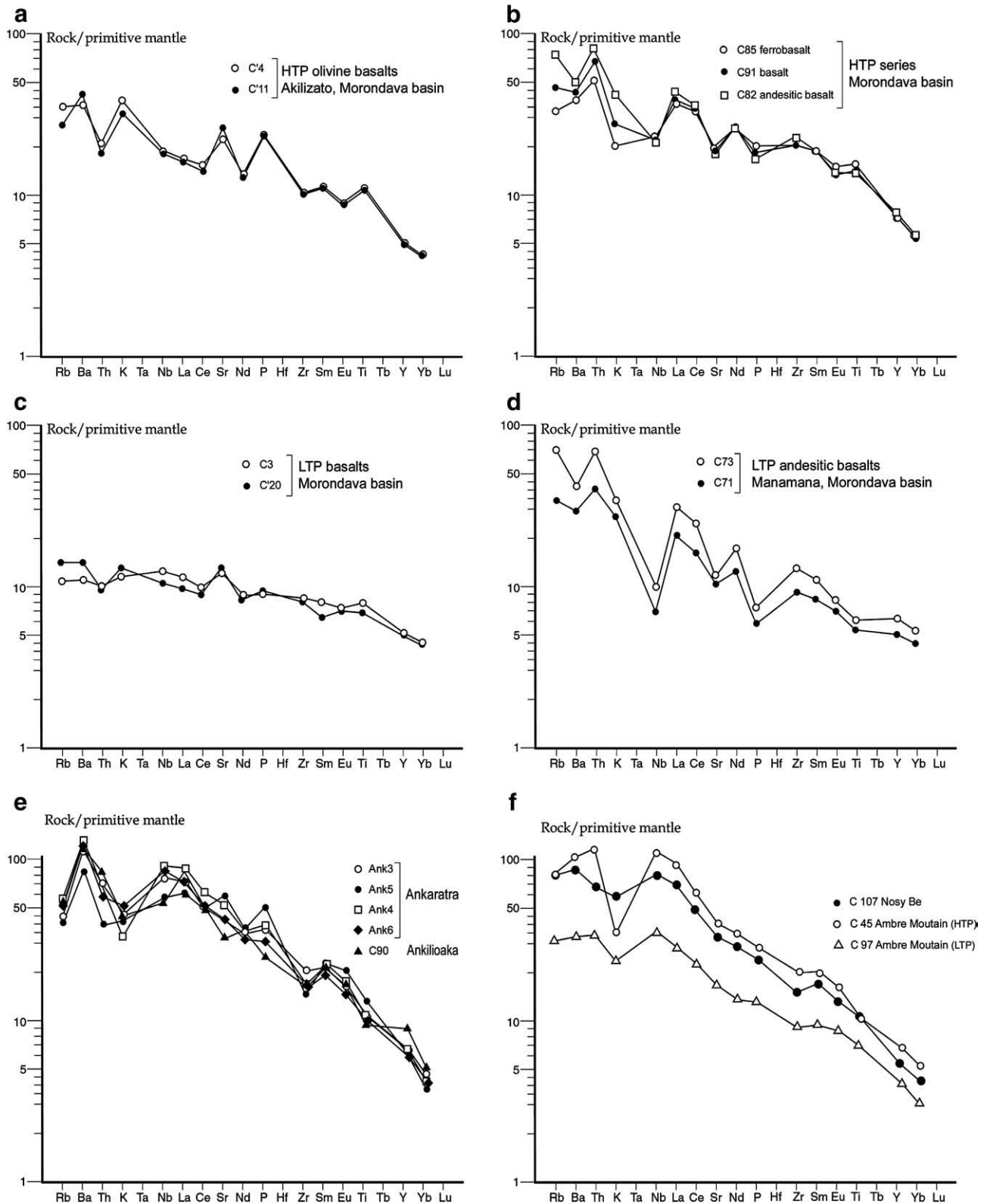


Fig. 4. Spidergrams for the volcanic formations of Madagascar (normalising values from Sun and McDonough, 1989). (a) HTP olivine basalts of Ankilizato, Morondava Basin, (b) HTP series of Morondava Basin, (c) LTP basalts of Morondava Basin, (d) LTP andesitic basalts of Manamana, Morondava Basin, (e) volcanic formations of Ankaratra and Ankiloaka, (f) volcanic formations of Ambre Mountain and Nosy Be.

for the reference age of 93 Ma are close to the primary magmatic values.

In the Upper Cretaceous Morondava Basin, the central subprovince displays the more depleted products (Fig. 6): LTP basalts (samples C'20,

C3) yield $Sr_i = 0.7031\text{--}0.7036$ and $\varepsilon_{Nd} = +7.5$ to $+7.7$ and HTP olivine basalts (C'11, C'4) $Sr_i = 0.7044\text{--}0.7051$ and $\varepsilon_{Nd} = +3.9$ to $+4.3$. Sr and Nd isotopic values of LTP basalts confirm that these are the most representative of the asthenospheric mantle beneath Madagascar. Only

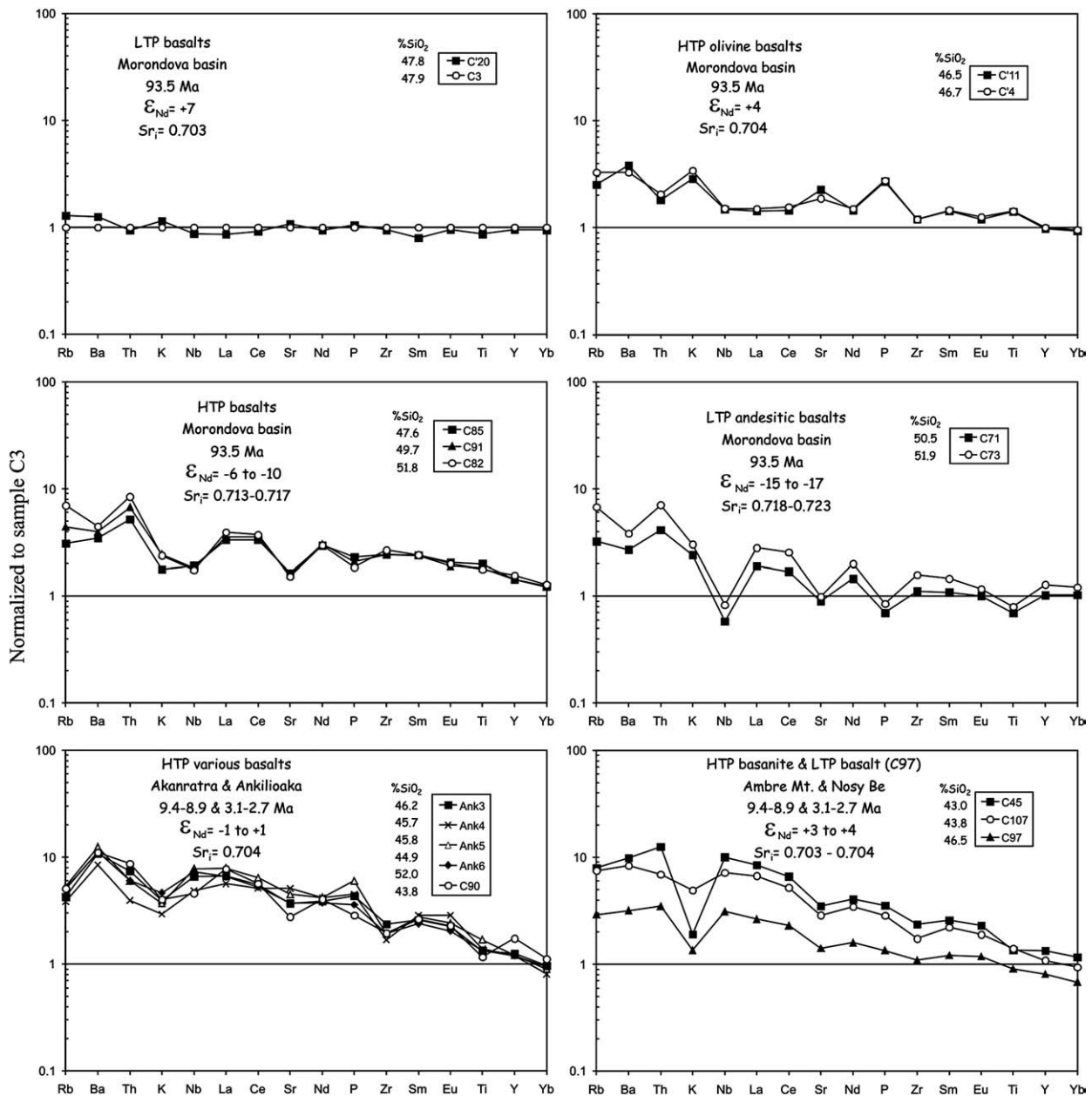


Fig. 5. Spidergrams of volcanic formations of Madagascar, normalised to the values for LTP basalt C3, which could be considered close to those of asthenospheric mantle beneath Madagascar.

one Nd T_{DM} model age can be calculated: this model age is 157 Ma. For rocks with eruptive ages around 93 Ma, this indicates a largely juvenile source with only a very low old continental input, if any.

By contrast, the southern subprovince is highly enriched (Fig. 6): $Sr_1 = 0.7133-0.7176$ and $\epsilon_{Nd} = -6.0$ to -9.0 in the HTP series, $Sr_1 = 0.7190-0.7228$ and $\epsilon_{Nd} = -15.5$ to -17.3 in LTP andesitic basalts. Paleoproterozoic T_{DM} model ages of 1570–1840 Ma for the HTP series, 2190–2270 Ma for LTP andesitic basalts are recorded. These old Nd T_{DM} model ages indicate an important participation of an old continental crustal component (early Paleoproterozoic or Archean in age) in the genesis of these volcanic rocks. Moreover, the different T_{DM} model ages recorded on both sides of the Bongolava–Ranotsara shear zone correlate with geologically contrasting terranes (Kröner et al., 1999; Collins and Windley, 2002).

The high Sr_1 and low ϵ_{Nd} values of the LTP suite of Manamana are currently interpreted as resulting from large crustal assimilation (Mahoney et al., 1991; Storey et al., 1997). However, this interpre-

tation cannot be extended to the two HTP series, because they are silica-undersaturated. This implies that an old continental signature is present within the lithospheric mantle, where crustal components have been incorporated in the past, most probably during the Pan-African or Eburnian subduction periods. We can then conclude that, with the possible exception of the LTP Manamana group, the Sr–Nd isotope systematics provides information on the mantle source compositions and that the incorporation of the local continental crust was weak.

The Cenozoic Ankaratra HTP province, Central Madagascar, displays (Fig. 6) a restricted range of compositions ($Sr_1 = 0.7040-0.7048$ and $\epsilon_{Nd} = +0.5$ to $+2.9$), suggesting a homogeneous enriched source, only slightly less enriched than the bulk silicate Earth (BSE) end-member.

The Miocene Ankiloaka province, related to the Tuléar fault zone, yields similar isotopic data ($Sr_1 = 0.7041$, $\epsilon_{Nd} = +0.8$) as Ankaratra, even closer to a BSE-like source (BSE), with no involvement of the nearby Manamana source.

Table 5

Sr–Nd isotopic data. Initial isotopic ratios have been recalculated for the age specified in the third column. T_{DM} Nd model ages were calculated after Nelson and DePaolo (1985), only for the samples having a $^{147}\text{Sm}/^{144}\text{Nd}$ ratio < 0.165.

Sample	Rock type	Age (Ma) (t)	Rb ppm	Sr ppm	$^{87}\text{Rb}/^{86}\text{Sr}$	$^{87}\text{Sr}/^{86}\text{Sr}$	$\pm 2\sigma$	$(^{87}\text{Sr}/^{86}\text{Sr})_t$	Sm ppm	Nd ppm	$^{147}\text{Sm}/^{144}\text{Nd}$	$^{143}\text{Nd}/^{144}\text{Nd}$	$\pm 2\sigma$	$(^{143}\text{Nd}/^{144}\text{Nd})_t$	$(\epsilon\text{Nd})_t$	T_{DM}
<i>Morondava</i>																
Central subprovince																
C'20	LTP basalt	93	8.8	271	0.0939	0.703688	0.000011	0.703564	2.8	11.3	0.1499	0.513002	0.000008	0.512911	7.66	157
C3	LTP basalt	93	6.8	250	0.0787	0.703194	0.000010	0.703090	3.5	12	0.1764	0.513008	0.000008	0.512901	7.46	/
C'11	HTP olivine basalt	93	17.2	565	0.0881	0.705227	0.000008	0.705111	5.0	17.5	0.1728	0.512842	0.000006	0.512737	4.26	/
C'4	HTP olivine basalt	93	22.4	468	0.1385	0.704595	0.000008	0.704412	5.1	18	0.1714	0.512823	0.000007	0.512718	3.90	/
Southern subprovince																
C85	HTP ferrobasalt	93	21	410	0.1483	0.713485	0.000010	0.713289	8.4	35.5	0.1431	0.512297	0.000008	0.512210	−6.02	1605
C91	HTP basalt	93	30	394	0.2205	0.71685	0.000009	0.716559	8.3	36.5	0.1375	0.512146	0.000005	0.512062	−8.90	1789
C82	HTP andesitic basalt	93	47.5	380	0.3621	0.718051	0.000010	0.717573	8.4	35.7	0.1425	0.512146	0.000008	0.512059	−8.96	1915
C71	LTP andesitic basalt	93	22	225	0.2833	0.719347	0.000010	0.718973	3.8	17.5	0.1313	0.511802	0.000013	0.511722	−15.54	2301
C73	LTP andesitic basalt	93	46	247	0.5398	0.723535	0.000009	0.722822	5.1	24	0.1285	0.511713	0.000008	0.511634	−17.25	2388
<i>Ankaratra</i>																
Ank3	HTP basalt	27.9	29	925	0.0907	0.704049	0.000008	0.704013	9.1	46.5	0.1177	0.512773	0.000010	0.512752	2.91	452
Ank4	HTP basalt	11.4	36	1124	0.0927	0.704202	0.000008	0.704187	9.7	50.5	0.1156	0.512755	0.000009	0.512746	2.40	469
Ank5	HTP basalt	17.2	26	1273	0.0591	0.704823	0.000008	0.704809	10.0	50	0.1210	0.512658	0.000009	0.512644	0.56	648
Ank6	HTP basalt	3.1	34	930	0.1058	0.704811	0.000008	0.704806	8.4	45	0.1122	0.512669	0.000004	0.512667	0.64	579
<i>Ankiloaka</i>																
C90	LTHP andesitic basalt	9.4	34.6	692	0.1446	0.704167	0.000010	0.704148	9.2	48.5	0.1147	0.512673	0.000006	0.512666	0.78	587
<i>Ambre Mt.</i>																
C45	HTP basanite	5	54	877	0.1781	0.703266	0.000011	0.703253	9.1	48.7	0.1124	0.512841	0.000009	0.512837	4.01	332
C97	LTP basalt	5	19.8	352	0.1627	0.70351	0.000008	0.703498	4.3	19.1	0.1346	0.512802	0.000008	0.512798	3.24	490
<i>Nosy Be</i>																
C107	HTP basanite	0.55	51	720	0.2049	0.703393	0.000008	0.703391	7.8	41.5	0.1137	0.512831	0.000005	0.512831	3.77	350

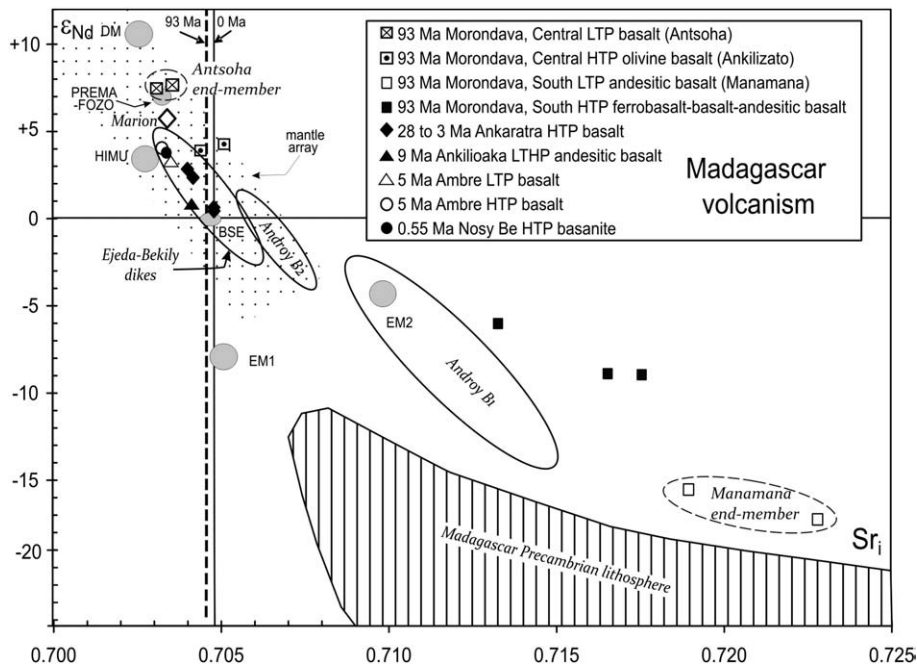


Fig. 6. ϵ_{Nd} vs. Sr isotopic ratios (recalculated to their eruption ages) of the analysed volcanic rocks of Madagascar. Marion (sample WJM-50) according to Mahoney et al. (1992), Androy B1 and B2 and Ejeda–Bekily dikes according to Mahoney et al. (2008). Madagascar Precambrian basement area calculated at 0 to 93 Ma from data of Tucker et al. (1999). The theoretical mantle reservoirs are also shown (grey circles/ellipses); the symbols cover the variations of the reservoir composition from 93 Ma to 0.5 Ma. DM = depleted mantle, PREMA = prevalent mantle, FOZO = focal zone, BSE = bulk silicate earth, HIMU = high- μ , EM1 = enriched mantle 1, EM2 = enriched mantle 2, dotted area = mantle array.

Ambre Mountain and Nosy Be Island volcanoes are more depleted ($Sr_i = 0.7033\text{--}0.7035$, $\epsilon_{Nd} = +3.2$ to $+4.0$) and likely to be derived from an alkali-enriched depleted mantle source (Fig. 6).

Such Sr–Nd isotopic variation for apparently similar rocks, emplaced in a short period within a restricted area, is exceptional.

7. Origins of primary magmas during the Cretaceous

Continental Flood Basalt (CFB) provinces have isotopic ratios different from mid-oceanic ridge basalts (Wilson, 1989). These characteristics, which are well portrayed in Madagascar, can be due to (a) interaction of asthenospheric liquids with an old crust, (b) melting of an enriched subcontinental lithospheric mantle, (c) upwelling of deep mantle plumes containing recycled components, (d) mixing of enriched and depleted mantle sources, or (e) any combination between these processes.

Crustal contamination, advocated by Mahoney et al. (1991) and Storey et al. (1997), cannot be a generally applicable hypothesis, especially in the case of silica-undersaturated suites. The subcontinental lithospheric mantle is assumed to be a rather thin (<150 km) reservoir of cold peridotite. There is growing evidence that this reservoir is not always anhydrous and depleted, but contains heterogeneous volumes of enriched peridotite, metasomatised and fertilised by aqueous fluids (Meibom and Anderson, 2003). As such, it provides an adequate “wet” reservoir for producing at fairly low temperatures small amounts of alkaline and potassic magmas (Black and Liégeois, 1993; Anderson, 1994, 1995) as well as large igneous provinces (Jourdan et al., 2009). In addition, the continental lithospheric mantle can generate mafic magmas (minettes, lamproites) with long-lasting enriched characteristics inducing isotopic signatures up to 0.720 in $^{87}Sr/^{86}Sr$ and -15 or -20 in ϵ_{Nd} (Tingey et al., 1991; Cartier et al., 2005; Gastal et al., 2005). Although less extreme, mafic rocks from the Jurassic Central Atlantic Magmatic Province (CAMP) can also have enriched Sr–Nd isotopic ratios that are mainly attributed to the lithospheric mantle, only small amounts of more felsic melts have been contaminated by the crust (Deckart et al., 2005; Jourdan et al., 2009).

In the case of CFB, the large volumes generated in a short period of time can be explained by the enriched nature (hence more fusible) of the continental lithospheric mantle, to mantle warming due to continental insulation (Coltice et al., 2007, 2009) and to decompression due to lithospheric reactivations (Liégeois et al., 2005). Extra-heat brought in by mantle plumes is not mandatory, as this supposed extra-heat in itself appears to be unable to generate LIPs in externally forced continental rifting (O'Neill et al., 2009).

The Cretaceous volcanism of Morondava is generally considered to be related to the Marion hot spot activity, at a time when it was relatively fixed under Madagascar (Nicollet, 1984; Mahoney et al., 1991; Storey et al., 1995; Meert and Tamrat, 2006) but alternative lithospheric models are now challenging this view. Our geological, trace element and Sr–Nd isotope data on this Cretaceous volcanic event as well as on the later Neogene volcanic events can be used as clues for the lithosphere versus deep mantle plume debate.

7.1. Incompatible element ratios and isotope compositions: a window into mantle sources

The compositions of the studied samples, which are mostly aphanitic, represent liquid chemistries. Any anomalies of distribution of the incompatible elements could be related to distinct, though not exclusive, processes: (a) liquid differentiation by mineral fractionation from a more primitive magma, (b) different compositions of the sources involved in the generation of primary magmas, and (c) chemical mixing of either solid sources, or primary magmas.

The chemical features of low HFSE (e.g., Nb) basaltic liquids may be interpreted in terms of contamination during ascent of the magmas in the crust, augmented by Fe–Ti oxide fractionation (Arndt et al., 1993). However, the tholeiitic to alkaline liquid lines of descent of the various

groups preclude any role played by Fe–Ti oxides (Melluso et al., 1997). The volcanic rocks of the Upper Cretaceous Morondava Basin bear mineralogical evidence of olivine + plagioclase saturation. This effect is weak to nil in the HTP family and becomes significant in the LTP family. In the series of incompatible elements, this fractionating mineral assemblage can affect only Sr and Eu that would be depleted at the same rates. Actually, REE compositions of all groups yield fractionated patterns characterised by a smooth shape. We conclude that the overall shapes of spidergrams are the consequence of the degree of partial melting and of the fractionation of major phases such as olivine or clinopyroxene but were not significantly modified by mineral fractionation that could generate anomalies in the spidergrams (Figs. 4 and 5), a similar case as MORBs. Thus, the selectively negative, or positive, anomalies of distribution should be a primary magmatic feature, providing a crude image of the mantle sources.

In particular, the measured ratios of highly incompatible elements will be very close to that of the source. These ratios have been determined for the different oceanic mantle end-members (Hofmann and Jochum, 1996) and can be used for comparison. In the diagram ($Th/La)_N$ vs. ($Th/Ba)_N$ (normalised to primitive mantle; Hofmann and Jochum, 1996; Fig. 7a), studied volcanic rocks that define two distinct groups: one above the PREMA source (similar to FOZO according to Zhu, 2007) and another rooted within an enriched mantle, more enriched than the usual EM2 field (Fig. 6). Such an enriched mantle is likely within a Palaeoproterozoic/Archaean lithosphere, as shown by the Sr–Nd isotopic composition of the Madagascar Precambrian crust (Tucker et al., 1999). Indeed, subduction events that are known to generate huge amounts of magmas, are also generating enriched metasomatic pockets in the lithospheric mantle. Further melting can produce very enriched magmas during post-collisional periods and later (Liégeois et al., 1998 and references therein). Elements with different compatibility (Nb and Rb are highly incompatible, Yb is moderately incompatible) separate the Morondava rocks from the others with a further subdivision within the former in three groups following the Ti content and the petrography (Diagram ($Nb/Yb)_N$ vs. ($Rb/Yb)_N$; Fig. 7b). In this case, ratios are much higher than the primitive mantle, indicating the role played by the degree of partial melting and by enriched pockets present in the lithospheric mantle.

In a first step, we will decipher the possible subcontinental lithospheric sources and evaluate the roles played by the different crustal and mantle sources. Their implication for the assembly of Gondwana terrains will be briefly examined further. In conclusion, we offer some speculations on the constitution of the different layers of the present lithosphere beneath Madagascar. The Upper Cretaceous volcanic formations display different trends marked by various negative and positive anomalies.

7.2. The Antsoha end-member

The LTP basalts, occurring around Antsoha, have relatively low incompatible element contents and the most depleted isotopic ratios, akin to the PREMA–FOZO pole in direction to the DMM end-member (Fig. 6). They define the Antsoha end-member. The flat pattern of their mantle-normalised spidergrams (Fig. 4c) look like E-MORB, the low level of trace elements coupled with very low Sr_i (93 Ma) and very high ϵ_{Nd} (93 Ma) cannot be accounted for by a mixture of the DMM end-member with other subcontinental sources.

Sr and Nd isotopes impose a recent enrichment in LILE, alkalis and LREE of a previously depleted mantle; an old enrichment would have largely modified these isotopic ratios with time, leading to much more enriched isotopic ratios (negative ϵ_{Nd} and higher Sr_i). This enrichment could result from a recent metasomatism of the lowermost lithospheric mantle but could also result from a low degree of partial melting. Considering the different constraints described above, this Antsoha end-member could lie at the base of the lithosphere, in the thermal boundary layer, recently cooled from the asthenosphere and

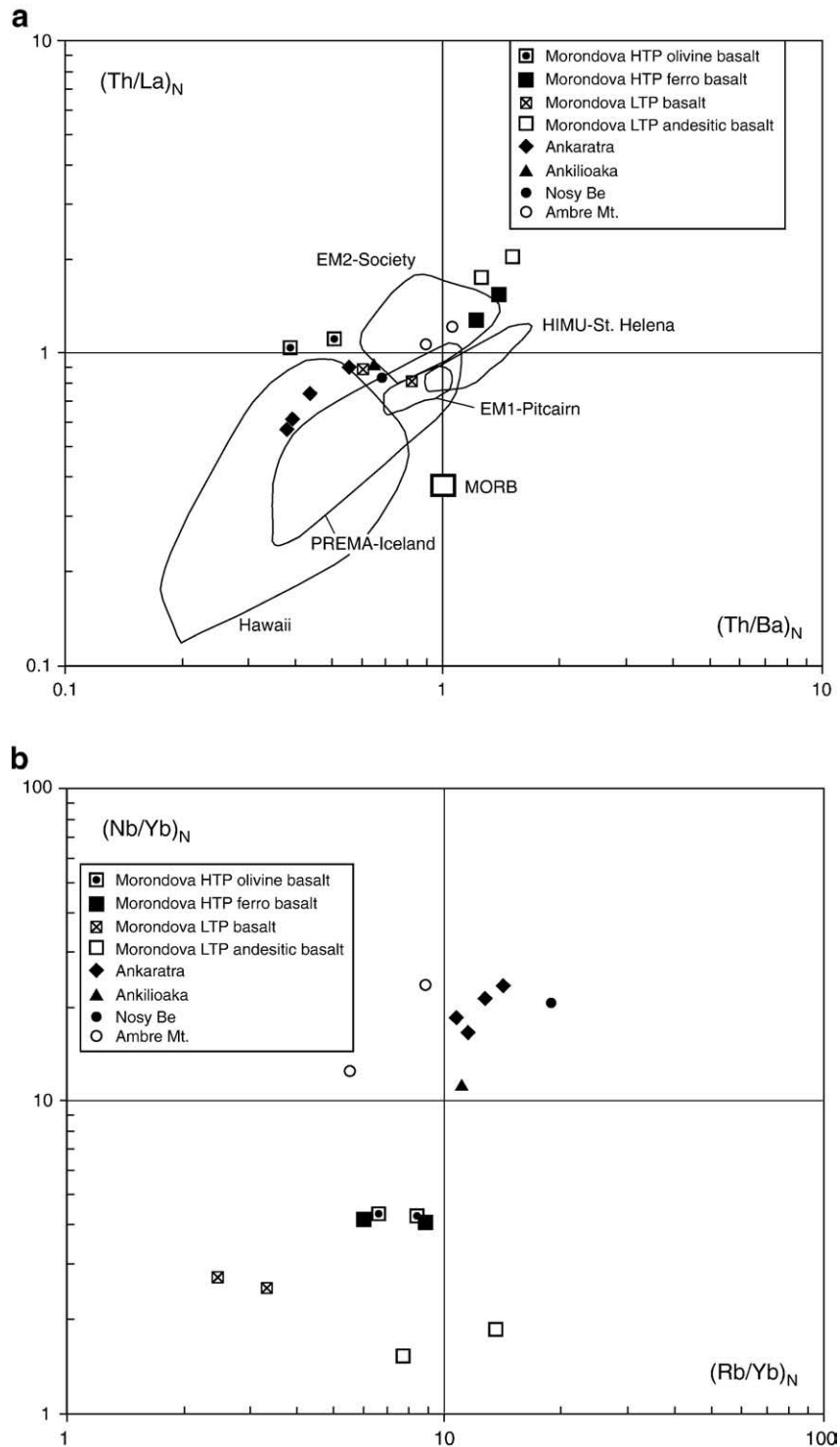


Fig. 7. (a) $(Th/La)_N$ vs. $(Th/Ba)_N$ diagram following Hofmann and Jochum (1996). Fields for HIMU, EM1, EM2, PREMA, MORB are also shown. (b) $(Nb/Yb)_N$ vs. $(Rb/Yb)_N$ diagram.

able to retain some enriched components (Black and Liégeois, 1993 and references therein).

Ankilizato HTP olivine basalts yield mantle-normalised spidergrams in which anomalies are the opposite to that of the Manamana andesitic basalts, i.e. positive anomalies and higher abundances of Sr, P and Ti and negative anomalies and lower abundances of Th, La, Ce, Nd, Zr. The only exception is the Nb negative anomaly that they share. In addition, low Sr_i (93 Ma) = 0.7044–0.7051 and high ε_{Nd} (93 Ma) = +3.9 to +4.3 preclude direct derivation of Ankilizato olivine basalts from the Manamana lithospheric source. They originated from a different, depleted, but

alkali-enriched subcontinental lithospheric mantle below the central area of the Morondava Basin, which was referred to as the Ankilizato end-member (Bardintzeff et al., 2001). However, now, considering the existence of the Antsoha end-member, it is more likely that the Ankilizato HTP olivine basalts are Antsoha magmas contaminated by older lithospheric products, the notion of Ankilizato end-member being not anymore used. This mixed source combines a prior depletion, marked by high ε_{Nd} (93 Ma) and more or less pronounced Nb, P, Ba, Sr and Ti negative anomalies, and by an ultimate alkali enrichment evidenced by high LILE abundances relative to HFSE.

7.3. The Manamana end-member

The Manamana andesitic basalts yield the most distinctive pattern, with high LILE and fairly low HFSE abundances, a sharply negative slope ($Rb/Yb)_N = 13$, steep negative anomalies in Nb, ($Nb/Yb)_N$ less than 2, Fig. 7b) (and probably Ta, which was not analysed) and P, and less pronounced negative anomalies in Ba, Sr and Ti (Fig. 4d). In non-subduction environments, a large Nb–Ta deficiency is considered an indicator of a continental crust component (Hawkesworth and Gallagher, 1993; Arndt et al., 1993).

The incompatible element compositions of Manamana LTP andesitic basalts match those of the CFB province of Karoo, South Africa (Duncan et al., 1984), for which a purely lithospheric source is proposed (Hawkesworth et al., 1999). The origin of negative anomalies is still a matter of discussion: they could be not primary, owing to crustal contamination at the magma chamber level (e.g. Arndt et al., 1993). Compared with the average compositions of upper and lower crust (Wedepohl, 1995), patterns of Manamana LTP andesitic basalts have more pronounced Nb negative anomalies, the same P normalised values and less negative Ti anomalies, which cannot be easily explained by simple magma–crust mixing processes.

Thus, the Manamana andesitic basalts could have originated from the subcontinental lithospheric mantle below the southern area of the Morondava Basin, having a chemical composition nearly identical to the subcontinental lithospheric mantle below the Karoo and Ferrar (Antarctica) CFB provinces. This enriched subcontinental lithospheric mantle, largely represented below the southern Gondwanan continents, will be referred to hereafter as the Manamana end-member (for location of Manamana in Madagascar, see Fig. 1). The Manamana end-member is the most enriched in terms of Sr–Nd isotopes, with Sr_i (93 Ma) = 0.7190–0.7228 and ϵ_{Nd} (93 Ma) = –15.5 to –17.3. It is more enriched than the classical EM2 pole and indicates the occurrence in the mantle source of an old crustal-like component, probably Paleoproterozoic to Archean in age (Nd T_{DM} model ages: 1570–2270 Ma). As the most enriched pockets present in the mantle are also its most fusible parts, they will contribute to the melt in a much higher proportion than their relative volume. Archean and Paleoproterozoic ages have been measured in zircon crystals of the basement below this area (Tucker et al., 1999; Kröner et al., 1999).

The role played by the Manamana end-member in the generation of the HTP series emplaced in the southern area of the Morondava Basin is illustrated by comparing their mantle (and C3) normalised spidergrams (Figs. 4 and 5). The HTP series differ from LTP Manamana andesitic basalts by higher levels of HFSE and comparable LILE contents, ruling out simple effect of different degrees of partial melting of the same source. Higher $(La/Yb)_N$ ratios could reflect the occurrence of garnet in the residue. Isotopically, the source of the HTP series is slightly less evolved with: Sr_i (93 Ma) = 0.7133–0.7176 and ϵ_{Nd} (93 Ma) = –6.0 to –9.0, still retaining a significant crustal-like enriched component. A mixture of 67% Manamana end-member (sample C73) + 33% Antsoha end-member (mean of samples C3 and C'20) can account for element and isotope compositions of HTP basalt sample C91. The HTP series can be explained by a combination of partial melting of a mixed source and subsequent mineral fractionation. Whatsoever, the Manamana mantle source must be physically distinct from the Antsoha mantle source.

7.4. Four mantle end-members

In addition to the here-defined lithospheric mantle source Manamana and Antsoha end-members, the DMM asthenospheric source and the Marion source, close to the PREMA end-member, should be considered as potential sources. It is commonly accepted that the Marion hot spot has triggered the magmatic episode 93 Ma ago but the corresponding mantle source is not evidenced by the observed volcanic products. Only the HTP series in the southern area

of Manamana could comprise this end-member mixed with subcontinental sources but obviously the Marion source is not needed here. The DMM asthenospheric source appears to have played a more significant role in the central area of Ankilizato.

Weaver (1991a,b) suggests the use of element/element ratio binary plots to distinguish the major chemical reservoirs (Fig. 8a). The four possible sources determined from the trace element compositions and the Sr–Nd isotope data used in this study define the Morondava quadrilateral, within which all the volcanic formations plot (Figs. 6 and 8b).

7.5. Comparison with other magmatic provinces of Madagascar

The variability of the possible mantle sources can be compared to the Seychelles–Comores hot spot, whose complexity is depicted by isotopic variations in space and time (Nougier et al., 1986; Späth et al., 1996; Deniel, 1998) or, as shown here, by a heterogeneous lithospheric mantle.

7.5.1. The Upper Cretaceous formations of the Majunga Basin (Table 6, Fig. 9a)

To the north of the Morondava Basin, about 500 km north of Ankilizato, the Majunga Basin shares common characteristics with Karoo continental detrital lower units overlain by shallow marine upper units, all of them being cut and overlain by basalts and andesitic basalts (Rasamimanana, 1996; Melluso et al., 1997). Melluso et al. (1997) distinguish four groups on the basis of TiO_2 , major and trace elements contents (Fig. 9b). Groups A, located along the eastern Antanimena range near Marovoay in the southwest of the basin, refers

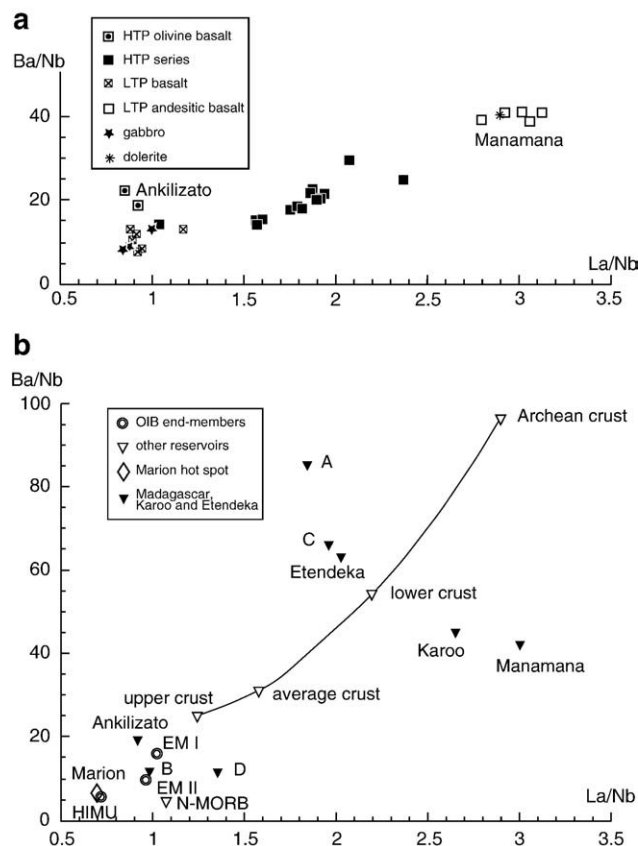


Fig. 8. Ba/Nb versus La/Nb plot. (a) The different groups of igneous formations in the Morondava Basin. (b) The possible sources of the volcanic formations in the Morondava Basin. Different mantle (N-MORB, EM I, EM II, HIMU, Weaver, 1991a,b) and crustal (Wedepohl, 1991, 1995) reservoirs, LTP Karoo (Duncan et al., 1984) and Etendeka basalts (Ewart et al., 1998) and end-members of the Majunga (A, B, C, D, Melluso et al., 1997) and Morondava (Manamana, Ankilizato) provinces are plotted for comparison.

to LTP andesitic basalts. It is thought to be derived from lithospheric sources enriched by previous subduction events, probably during the 600 Ma old Pan-African orogeny. Group B is located at Bongolava in the central area of the basin, and is composed of high-Ti medium-P basalts, characterised as low-K/Nb. This group is volumetrically the most abundant. Bulk-rock compositions are strikingly similar to some formations of the Deccan flood basalts. Group B was derived from LILE-depleted mantle sources, which are considered to be lithospheric because their incompatible element contents and ratios are unlike those of MORB. Group C is located along the western Antanimena range, the south westernmost part of the basin, and corresponds to HTP andesitic basalts. Group D is heterogeneous and located in the northern part of the basin, comprising HTP basalts characterised by high and increasing levels in TiO₂, Nb, Sr and Zr from D1 to D3 subgroups.

Sr isotope ratios, low in the B group (0.7039), increase in the D group from 0.7050 to 0.7053, and reach the high values of 0.7070 to 0.7080 in the A and C groups. Melluso et al. (1997) conclude that the volcanic rocks came from variably enriched sources. The groups defined by Melluso et al., with the exception of the B group, can be compared with those defined in the Morondava Basin. However, their mantle-normalised spidergrams differ markedly. In the case of the A and C groups with high Sr isotopic ratios, the patterns are roughly parallel and weakly fractionated, with a large positive anomaly in Ba and a clear negative anomaly in Nb. They could be derived from different, yet small, degrees of

partial melting of another lithospheric source, the Antanimena end-member that is completely different from the Manamana and Antsoha end-members defined in the Morondava Basin. The trace element and high Sr isotope ratios of the Antanimena end-member resemble LTP basalts of the Etendeka CFB province (Ewart et al., 1998).

The B group of Bongolava has rather exotic compositions. The abundances of incompatible elements from Nb to Lu are identical to the C group, but LILE are heavily depleted by a factor of 5 (Rb, Ba) to 15 (K, which yields chondritic normalised values). The cause for such an important depletion remains unknown. Low Sr isotope ratios preclude any alteration in crustal conditions. Melluso et al. point out that similar formations are known in some Deccan traps in India, which would imply that the subcontinental lithosphere 88 Ma ago was, at least in part, the same below Bongolava, the central part of the Majunga Basin, and the Deccan.

The D group with intermediate Sr isotopic ratios displays patterns grossly similar to those of Marion, with the exceptions of K and Nb negative anomalies. A possible explanation of the intermediate values displayed by Sr isotope ratios and spidergrams could be that the D group rocks were derived from a source constituted by a mixture of the Antanimena end-member and the Marion source. Thus, the heterogeneous lithosphere below the Majunga Basin was not identical to the one below the Morondava Basin.

7.5.2. The Upper Cretaceous formations of southern and eastern coasts

The southern coast of Madagascar has been extensively studied, because the major volcanic feature, the Volcan de l'Androy, was postulated to be situated 88 Ma ago above the hypothetical focal point of the Marion hot spot. Mahoney et al. (2008) point out a thick sequence of interbedded predominant basalt and rhyolite. Two groups of lower and upper basalts are defined (Rasamimanana, 1996; Table 6). The Androy upper basalts unit of Rasamimanana (1996) corresponds to the group B1 of Mahoney et al. (2008). They are medium-Ti (1.95–2.81 wt.% TiO₂) and medium-P (0.28–0.45 wt.% P₂O₅). Their mantle-normalised spidergrams (Fig. 9a) resemble those of Manamana andesitic basalts. Their isotopic ratios, $0.709 < Sr_i (88 \text{ Ma}) < 0.715$ and $-13.2 < \epsilon_{Nd} (88 \text{ Ma}) < -2.4$ (Mahoney et al., 2008) are less enriched than the Manamana end-member (Fig. 6). The authors consider the group B1 as having almost certainly assimilated continental crust.

The Androy lower basalts unit, or alternatively the group B2, are HTP (3.24–3.65 wt.% TiO₂, 0.4–0.5 wt.% P₂O₅). Their slightly fractionated spidergrams have weak or no anomalies. Though their trace element contents could resemble those of Marion basalts, Sr_i (88 Ma) values of 0.7058–0.7073 and ϵ_{Nd} (88 Ma) values of +0.6 to –2.4 differ so strikingly that Storey et al. (1997) consider that this group represent alkaline liquids derived by small degrees of melting of the continental lithospheric mantle. Though the Volcan de l'Androy was active at the presumed focal point of the Marion hot spot, all its source signatures should be all attributed to the subcontinental lithospheric mantle. Its most enriched sample is, however, less enriched than the Manamana end-member and resembles the source of Neogene volcanic formations (see below).

Along the eastern coast as well as within the Ejeda–Bekili dike swarm (Mahoney et al., 1991), located in between Manamana and Volcan de l'Androy, the magma compositions extend between PREMA and BSE poles, in a manner similar to that of the Neogene Ankaratra, Ankilioaka, Ambre and Nosy Be volcanisms.

8. Origins of primary magmas during the Neogene

The Neogene volcanic activity in Madagascar differs strongly from the Cretaceous CFB event, by the build up of central volcanoes and outpouring of comparatively less voluminous lava flows. Here we have studied the Ankaratra, Ankilioaka, Ambre Mountain, and Nosy Be Neogene basalts. The less silicic Ankaratra rocks (28 to 3 Ma) have isotopic ratios, $Sr_i = 0.7040\text{--}0.7048$ and $\epsilon_{Nd} = +0.5$ to +2.9 (Fig. 6), tending to the BSE (Bulk Silicate Earth) end-member. This suggests

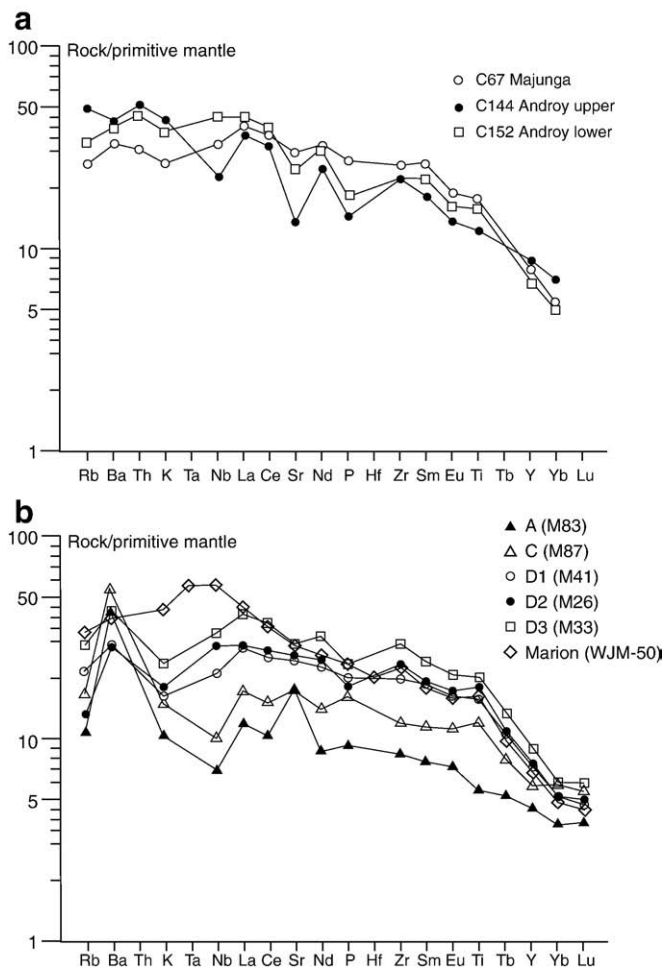


Fig. 9. (a) Spidergrams of the volcanic formations of Majunga and Androy (normalising values from Sun and McDonough, 1989). (b) Spidergrams for the volcanic formations of Morondava Basin (A, C and D group, according to Melluso et al., 1997) and of Marion (sample WJM-50, Storey et al., 1997) (normalising values from Sun and McDonough, 1989).

Table 6

Selected chemical analyses of representative lavas from other provinces in Madagascar: Majunga (C67), Androy (upper C144, lower C152). LOI for Loss On Ignition.

	Majunga C67	Androy upper C144	Androy lower C152
<i>wt.%</i>			
SiO ₂	49.90	51.20	48.00
TiO ₂	3.95	2.76	3.53
Al ₂ O ₃	13.42	13.25	12.73
Fe ₂ O ₃	14.00	14.01	13.73
MnO	0.18	0.20	0.18
MgO	4.64	3.76	5.75
CaO	8.60	8.30	10.55
Na ₂ O	2.85	2.43	2.35
K ₂ O	0.79	1.32	1.15
P ₂ O ₅	0.63	0.34	0.41
LOI	0.98	1.83	1.36
Total	99.94	99.49	99.74
<i>ppm</i>			
Rb	16.7	31.5	21.5
Sr	620	290	512
Ba	235	298	280
Sc	21.5	28	29
V	355	350	390
Cr	26	15	113
Co	43	42	47
Ni	54	20	92
Y	37	40	32
Zr	292	250	250
Nb	23.6	16.2	32
La	29	26	32
Ce	67	59	73
Nd	45	34	43
Sm	11.7	8.2	9.9
Eu	3.22	2.35	2.7
Dy	7.6	7.5	6.7
Er	3.3	4	3.1
Yb	2.62	3.39	2.42
Th	2.7	4.4	4

that the Neogene Ankaratra volcanic formations did not originate in the same sources as the Cretaceous CFB.

The less silicic Ankilioaka rocks (9 Ma) have Nb contents higher than those in any Upper Cretaceous formations of the nearby Morondava Basin, suggesting another mantle source. Isotopic ratios, $Sr_i = 0.7041$ and $\epsilon_{Nd} = +0.8$, are close to the BSE end-member. This suggests that the Upper Miocene Ankilioaka volcanic formations originated from the same source as Ankaratra.

The younger HTP basanite and LTP basalt families from both Ambre Mountain and Nosy Be have chemical features similar to those of the Ankaratra and Ankilioaka basalts. Isotopic ratios are clustered in the range of 0.7033–0.7035 for Sr_i , and of +3.2 to +4.0 for ϵ_{Nd} , indicating a more depleted source than at Ankaratra and Ankilioaka but on the same trend as that defined by the Ankaratra basalts (Fig. 6).

The mantle-normalised spidergrams of all Neogene volcanic formations have the same general shape marked by a pronounced negative anomaly in K. The large K trough can be attributed to the presence within the mantle source of K-bearing refractory minerals, such as phlogopite and perhaps potassic richterite. From what is currently known about the stability limits of hydrous phases in the mantle, the negative K anomaly can indicate relatively shallow depths for partial melting, i.e. within the only slightly enriched lower part of the thermal boundary layer (TBL) of the subcontinental lithosphere. It should be noted that the spidergrams of volcanic formations of the nearby Comores archipelago, i.e. the Neogene La Grille type of Späth et al. (1996), display the same features, attributed to the partial melting of an amphibole-bearing heterogeneous source representative of the sub-Comorean mantle, comprising a mixture of materials within the lithosphere, with a limited contribution from a “plume” component (Späth et al., 1996; Deniel, 1998).

The Madagascar Neogene volcanism has limited variations in geochemistry and Sr–Nd isotopic signature that can be explained by the mixing of two components, of which the depleted one could be the Antsoha end-member and the enriched one the BSE or a pole beyond. It must be noted that the shorter trend shown by the Neogene volcanism is not superimposed on the Cretaceous trend. This suggests that the enriched pole does not correspond to the Manamana end-member. The assumed enriched pole for the Neogene volcanism should be less enriched in ^{87}Sr , for the same ϵ_{Nd} .

9. Origin of the Madagascar Meso-Cenozoic volcanism: plume vs. lithosphere

9.1. The Marion plume hypothesis is not supported

The Marion oceanic island, in the oceanic part of the Antarctic plate, south of the South West Indian Ridge (SWIR) is considered the present trace of the Marion mantle plume (hot spot) activity (Mahoney et al., 1992; Storey et al., 1997). Plate reconstructions place Madagascar over the Marion hot spot in the 120–80 Ma interval (Duncan et al., 1989). According to Storey et al. (1995), the focal point of the hot spot 93–88 Ma ago was located beneath the Volcan de l'Androy, in the southern edge of the island, and the mantle plume was instrumental in causing continental break-up between Madagascar and India.

On the Marion Island, transitional basalts resemble the Cretaceous HTP series of Madagascar in terms of SiO₂, TiO₂ and P₂O₅, but are higher in alkalis (Na₂O + K₂O > 4.3 wt.% in Marion, <3.6 wt.% in the HTP series). The mantle-normalised spidergrams (Fig. 9b) are characterised by a fractionated pattern, with (Rb/Yb)_N = 7.4, and a bell shape, with the highest normalised values (60) for Nb and Ta. Radiogenic isotope characteristics, ϵ_{Nd} ranging from +5.7 to +7.4 and Sr_i from 0.7029 to 0.7034 (Mahoney et al., 1992), are close to the PREMA end-member defined by Zindler and Hart (1986), which can be considered as a complex mixture of DMM end-member + (EM I + EM II + HIMU) OIB end-members.

Geochemically, this plume model could account for the Cenozoic Ambre Mountain and Nosy Be volcanic formations, but, at that time, the advocated plume was far away. For the Cretaceous volcanism, when the plume would be in the vicinity, the geochemistry and Sr–Nd isotopes cannot be reconciled with a plume.

As a consequence, we prefer a model in which the different mantle sources are located in the lithospheric mantle, maybe at the lithosphere–asthenosphere boundary for the Antsoha end-member. Indeed, the base of the TBL could stock the heterogeneities existing in the convecting asthenosphere (Black and Liégeois, 1993). This model must be compatible with the Madagascar lithospheric composition and a cause for the partial melting of the lithospheric mantle must be proposed.

9.2. Composition of the Madagascar lithosphere

9.2.1. Displaced terranes in the continental crust of Madagascar

The continental crust of Madagascar is made up of at least two discrete displaced terranes, that were welded during consolidation of the Gondwana supercontinent at the end of the Pan-African orogeny (Shackleton, 1996; Yoshida et al., 1999; Collins, 2006). West Madagascar is part of the Neoproterozoic Vohibory belt, which includes a juvenile assemblage of pillow-bearing greenstones, gabbros and chromite peridotites. U–Pb zircon age determinations (De Wit et al., 1998) indicate scarce remnants of 2520 Ma Archean orthogneisses and younger metasedimentary paragneisses. A 722 Ma felsic metavolcanic unit contains detrital zircons ranging in age between 1700 and 1300 Ma. The youngest metasediments must have been deposited at the onset of their deformation 647 to 607 Ma ago. The central area of the Vohibory belt was remobilised by the major

NW–SE trending Bongolava–Ranotsara shear zone, with its left lateral movement being active 550 to 520 Ma ago (Rolin, 1991). East Madagascar is composed of reworked Archean to Paleoproterozoic and Mesoproterozoic metamorphic formations (Shackleton, 1996; Kröner et al., 2000; Collins, 2006). Between the two major terranes, a complex thrust and shear zone is exposed.

Phanerozoic sediments were deposited onto this complex supra-crustal assemblage, and subsequent volcanic formations were produced from the partial melting of and/or intruded the different lithosphere pieces. The Neoproterozoic Vohibory belt is now covered by the Morondava Phanerozoic Basin and also forms the southern coast of Madagascar. The Manamana volcanic rocks representing the lithospheric end-member are ubiquitous south of the Bongolava–Ranotsara shear zone, whereas those matching the Antsoha end-member are present only to the north. As they have distinct compositions, the 550 to 520 Ma Bongolava–Ranotsara shear zone should then correspond to a major boundary between two discrete Neoproterozoic terranes, each displaying its own continental crust and subcontinental mantle lithosphere.

The Archean to Paleoproterozoic basement is covered by the Majunga Basin and constitutes most of the northern and eastern coasts. Accordingly, the lithosphere sources in these areas differ strikingly from those for the Morondava Basin and the southern coast. They could be derived from the same enriched mantle source, that suffered LILE depletion at least 3 Ga ago, i.e. during the Archean.

9.2.2. The subcontinental upper mantle below Madagascar

The lower limit of the lithospheric upper mantle is given by the ca. 1300 °C isotherm, corresponding to the peridotite dry solidus (for definitions and reviews, see McKenzie and Bickle, 1988; Black and Liégeois, 1993). Just below the crust, the mechanical boundary layer is defined by a thickness approximating the elastic thickness and its base corresponds to the brittle–ductile transition of olivine at the depth of the 600 °C isotherm. This layer is probably completely isolated from the convecting mantle and so could acquire specific isotopic and chemical compositions. The thermal boundary layer has temperatures increasing progressively with depths from 600 to 1300 °C and constitutes a transition to the asthenosphere. Mantle materials from below are added to this fluctuating region when lithosphere cools, or are removed from it when it is subjected to stretching and is heated by an ascending convective cell (Black and Liégeois, 1993; Maruyama et al., 2007). The thermal boundary layer can, therefore, have a composition similar to the asthenosphere (it is actually a frozen asthenosphere). It is also able to retain some enriched material. Generally such enrichments are young, implying that they are geochemically visible but less through radiogenic isotopes that have not enough time to decay significantly.

9.2.3. The lithospheric sources of the Malagasian volcanism

The Cretaceous Malagasy volcanism has two end-members that, through mixing, can account for the other volcanic manifestations of the same age. The depleted Antsoha end-member is considered to lie at the base of the lithosphere, in the thermal boundary layer, recently cooled from the asthenosphere and able to retain some enrichments. The Manamana end-member has the composition of an old enriched lithospheric mantle, enriched in LREE and in LILE for a long time, accounting for the strongly enriched signature of this end-member. Nd T_{DM} model ages between 1.6 and 2.4 Ga indicate that at least a part of this enrichment has to be Archean in age. Palaeoproterozoic and Pan-African enrichments are also possible. Enrichments probably occurred through metasomatism of the lithospheric mantle during subduction event(s). This implies that the Manamana end-member is located within the mechanical boundary layer (MBL) part of the Archean lithosphere, most probably reworked later, especially during the Neoproterozoic (Paquette et al., 1994; Tucker et al., 1999). Madagascar, prior to the Mesozoic drifting, was part of the Mozambique Belt and was

close to Tanzania where Archean and Palaeoproterozoic gneisses have been reworked during a Neoproterozoic (Pan-African) high-grade event (Vogt et al., 2006). When looking at the geographical position relative of the Antsoha depleted end-member and the Manamana enriched end-member, each on different sides of the major Bongolava–Ranotsara shear zone, a parallel can be made with the basalts from the Central Atlantic Magmatic Province (CAMP) at c. 200 Ma where they are strongly depleted in Guyana, South America ($Sr_i = 0.704$, $\epsilon_{Nd} = +5$) and more enriched in Guinea, Africa ($Sr_i = 0.705$ – 0.710 , $\epsilon_{Nd} = +0.5$ to -5.5) (Deckart et al., 2005).

The Neogene Malagasy volcanism is smaller in volume but more homogeneous in composition. It is also less widespread. Its source would be the result of mixing between the equivalent of the Antsoha depleted end-member with an enriched end-member close to BSE or beyond but different from the Manamana end-member. Its Nd T_{DM} model age, varying from 330 to 650 Ma, suggests that this enriched component lies above the Antsoha source but lower than the Manamana end-member, i.e. in the upper part of the TBL.

9.3. Origin of the partial melting of the Malagasian lithosphere

The temporal association of the two Cretaceous Antsoha and Manamana end-members and their mixing suggests that the Antsoha deeper TBL source brought up the heat needed to melt the Manamana MBL shallower source. Reactivation of shear zones in response to far-distant stress has been proposed for triggering of alkaline intraplate magmatism (Black et al., 1985; Liégeois et al., 1991, 2005; Black and Liégeois, 1993; Bonin, 2004). Major shear zones are characterised by a higher heat flow due to a thinner lithosphere (e.g. Teyssier and Tikoff, 1998) as it is the case in rifts, even if displacement is weak or null (Nicolas and Boudier, 2008). This could be due to linear lithospheric delamination during the reactivation of the shear zone (Liégeois et al., 2003). Recent reevaluation of thermal diffusivity of rocks with temperature suggests that strain heating can play a significant role in triggering crustal and mantle anatexis (Whittington et al., 2009). In any case, this occurs preferentially along domains with contrasted lithosphere where small-scale convection is enhanced (Dumoulin et al., 2004), corresponding to the “edge effect” of King and Anderson (1998). It must be noted that the process is self-enhancing (Dumoulin et al., 2004): the reactivation generates a linear delamination favouring partial melting that in turn favours movements, delamination and partial melting above.

The stress field needed for the reactivation can be related to the general plate process affecting the region (Patriat and Achache, 1984). The initial break-up occurred at c. 175 Ma with the spreading of a true ocean between SE Africa and Madagascar–Antarctica (Somali and Mozambique Basins) corresponding to the break-up of West and East Gondwana (Schettino and Scotese, 2005). The Somali Basin and the Davies Ridge, west of Madagascar, became inactive at c. 120 Ma (Marks and Tikku, 2001). If India–Madagascar moved during that period on more than 1400 km relative to Africa, the width of the oceanic basins was never important (Melluso et al., 2009), as demonstrated by various common tetrapod families (Ali and Aitchison, 2008) and plate tectonic reconstructions (Fig. 10; Stampfli and Borel, 2002). The definitive break-up between Madagascar and India occurred at c. 85–90 Ma. Just after 96 Ma, reorganisation of the oceanic plates occurred in the area, including fracture zones around the Bouvet triple junction, the South–West Indian Ridge propagating eastward, south of Madagascar (Marks and Tikku, 2001). The 99–96 Ma period is also the time when the spreading movement in the Indian Ocean had changed to N–S direction (Rotstein et al., 2001). Thus, strong lithospheric stress was applied to the Madagascar lithosphere at c. 93 Ma, the time of the Malagasian volcanism that occurred on both margins of the great island.

We propose that this major regional stress was able to reactivate the preexisting shear zones, generating linear delamination along

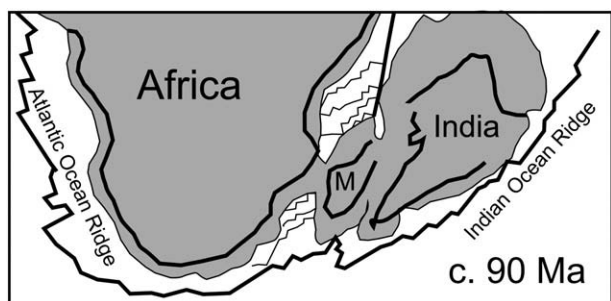


Fig. 10. Paleogeographical reconstruction at c. 90 Ma showing the relative position of Madagascar relatively to Africa and Greater India, just before the break-up between the two latter (adapted from Stampfli and Borel, 2002). Note that while the rifting between Africa and Madagascar/India occurred since 175 Ma, the oceanic domains are still small.

them with partial melting at the lithosphere–asthenosphere boundary (the Antsoha end-member). When the tectonic movement, even limited, allowed the upward movement of the magma; a minor part reached the surface, with the larger part remaining at depth within the MBL and provoking its partial melting (Manamana end-member). Immediately as the extension began towards the drifting of India, the stress in the Madagascar lithosphere decreased, explaining the short-lived Malagasian Cretaceous volcanism.

During the Cenozoic, volcanism occurred several times between 28 and 0.55 Ma. All these volcanic events share a similar Sr–Nd signature between the Antsoha end-member and the BSE signature, without the participation of the Manamana enriched end-member. The BSE-like member can lie within the TBL, lower part of the lithospheric mantle and this volcanism can be seen as the result of the mixing of the asthenosphere and the lower part of the TBL. This suggests that, during the Neogene, the mobilisation of the Antsoha source and the tectonic reactivation was not strong enough to melt the upper, colder lithospheric mantle. It should be noted that 28 Ma is the age of the generation of the main central thrust (MCT) in the Himalaya and 9 Ma the age of its reactivation (Yin, 2006). These events, characterised by more intense stress applied to the Indo-Australian plate, could induce tectonic repercussion on the eastern oceanic part of the African plate. Likewise, the shift in the direction of absolute motion of the Pacific plate evidenced by the bend of the Hawaiian–Emperor chain can be interpreted as a consequence of the India–Eurasia collision (Patriat and Achahe, 1984). They triggered volcanism along major discontinuities, as in Madagascar, but with less volume than during the Cretaceous opening period. The upper colder part of the lithospheric mantle (MBL) was not affected by the process, except in brittle conditions, allowing the ascent of the TBL/asthenospheric magmas.

10. Summary and conclusions

After the consolidation of the Gondwana supercontinent at the end of the Pan-African orogeny, the subcontinental lithosphere of Madagascar was composed of various pieces of upper mantle differing by their compositions and histories, including Archean and Paleoproterozoic blocks. Subsequently, the region was affected by four discrete episodes of contrasting durations: (a) cooling and thickening for ca. 500 Ma, corresponding to the Paleozoic and most of the Mesozoic, (b) stretching, slight warming and thinning in a short interval of time (93–88 Ma) during the Turonian (Upper Cretaceous) accompanied by volcanism, (c) cooling and thickening from about 60 Ma ago till the Neogene and, finally, (d) during the Neogene, limited tectonic reactivation with minor (?) volcanism.

The Upper Cretaceous (Turonian) episode was marked by continental break-up between Madagascar and Greater India, accompanied by intense volcanic activity involving lithosphere and asthenosphere sources all over the Island of Madagascar.

In the central area of the basin, near Ankilizato, the low titanium–phosphorus (LTP) basalts are slightly more depleted than the PREMA–FOZO reservoir ($Sr_i = 0.7033$, $\epsilon_{Nd} = +7.5$) and could represent a slightly enriched asthenosphere or a mixing between a depleted asthenosphere and the base of the lithosphere (TBL, thermal boundary layer) partly enriched. These basalts represent the depleted Madagascar source, the Antsoha end-member. The Ankilizato HTP olivine basalt ($Sr_i = 0.7048$, $\epsilon_{Nd} = +4$) results from the same source contaminated by the enriched Manamana end-member ($Sr_i = 0.7200$, $\epsilon_{Nd} = -16$), represented by the Manamana LTP andesitic basalts. The latter are located 200 km to the south, on the other side of a major shear zone. In the same area, the HTP basalt series is less extreme in its enrichment ($Sr_i = 0.716$, $\epsilon_{Nd} = -8$). The Manamana end-member corresponds to the upper part of the lithospheric mantle (mechanical boundary layer, MBL), older and colder, being melted by the Antsoha-derived melts, which they partially mixed with. It resembles the lithospheric source of Karoo and Ferrar (Antarctica) CFB provinces and could represent a large part of the mechanical boundary layer below the southern Gondwanian continental fragments.

These results are difficult to reconcile with the classical mantle plume model. We interpret the upper Cretaceous Malagasian volcanism as resulting from the reactivation of lithospheric scale shear zone due to the oceanic plate reactivation that occurred during this period and has eventually led to the continental break-up between Madagascar and India.

After this episode, a different near-BSE source was incorporated into the thickening thermal boundary layer, which was remobilised later, during the less intense and less voluminous Neogene volcanic activity but that lasted from 28 to 0.5 Ma. This reactivation is tentatively correlated with the main events that occurred at the time in the Himalayas and that could trigger low-intensity reactivation in the eastern oceanic part of the African plate.

Acknowledgments

J. Cotten and J.-C. Philippet, at the Université de Bretagne Occidentale at Brest, and R. Coquet at Orsay are thanked for their careful bulk-rock geochemical analyses and K–Ar age measurements. L. Daumas and G. Roche are thanked for drawings. A.R. McBirney is thanked for useful remarks. Careful reviews by two anonymous reviewers have greatly improved the manuscript. This study was made possible through funding by the CAMPUS project on the “Rifting malgache” supported by the French Ministry of Cooperation and Development (2000–2003), and further help by Aupelf-Uref and Papeteries de Madagascar.

References

- Ali, J.R., Aitchison, J.C., 2008. Gondwana to Asia: plate tectonics, paleogeography and the biological connectivity of the Indian sub-continent from the Middle Jurassic through latest Eocene (166–35 Ma). *Earth Science Reviews* 88, 145–166.
- Anderson, D.L., 1994. The sublithospheric mantle as the source of continental flood basalts – the case against the continental lithosphere and plume head reservoirs. *Earth and Planetary Science Letters* 123, 269–280.
- Anderson, D.L., 1995. Lithosphere, asthenosphere and perisphere. *Reviews of Geophysics* 33, 125–149.
- Arndt, N.T., Czamanske, G.K., Wooden, J.L., Fedorenko, V.A., 1993. Mantle and crustal contributions to continental flood volcanism. *Tectonophysics* 223, 39–52.
- Bardintzeff, J.M., Leyrit, H., Guillou, H., Guille, G., Bonin, B., Giret, A., Brousse, R., 1994. Transition between tholeiitic and alkali basalts: petrographical and geochemical evidences from Fangataufa, Pacific Ocean, and Kerguelen, Indian Ocean. *Geochemical Journal* 28 (6), 489–515.
- Bardintzeff, J.M., Bonin, B., Rasamimanana, G., 2001. The Cretaceous Morondava volcanic province (West Madagascar): mineralogical, petrological and geochemical aspects. *Journal of African Earth Sciences* 32 (2), 299–316.
- Bellon, H., Quoc Buu, N., Chaumont, J., Philippet, J.C., 1981. Implantation ionique d'argon dans une cible support. Application au traçage isotopique de l'argon contenu dans les matériaux et les roches. *Comptes Rendus de Académie des Sciences, Paris* 292, 977–980.
- Besairie, H., 1972. Géologie de Madagascar, 1. Les terrains sédimentaires. *Annales Géologiques de Madagascar* 35, 1–463.
- Besairie, H., Boulanger, J., Brenon, P., Emberger, A., de Saint-Ours, J., 1957. Le volcanisme à Madagascar. *Travaux du Bureau Géologique, Madagascar* 83.

- Black, R., Liégeois, J.P., 1993. Cratons, mobile belts, alkaline rocks and continental lithospheric mantle: the Pan-African testimony. *Journal of the Geological Society of London* 150, 89–98.
- Black, R., Lameyre, J., Bonin, B., 1985. The structural setting of alkaline complexes. *Journal of African Earth Sciences* 3, 5–16.
- Bonin, B., 2004. Do coeval mafic and felsic magmas in post-collisional to within-plate regimes necessarily imply two contrasting, mantle and crustal, sources? A review. *Lithos* 78, 1–24.
- Bumby, A.J., Guiraud, R., 2005. The geodynamic setting of the Phanerozoic basins of Africa. *Journal of African Earth Sciences* 43 (1–3), 1–12.
- Cartier, G., Lorand, J.P., Liégeois, J.P., Fornari, M., Soler, P., Carlotto, V., Cardenas, J., 2005. Potassic-ultrapotassic mafic rocks delineate two lithospheric mantle blocks beneath the southern Peruvian Altiplano. *Geological Society of America* 33 (7), 601–604.
- Coffin, M.F., Rabinowicz, P.D., 1987. Reconstruction of Madagascar and Africa: evidence from the Davie fracture zone and Western Somali basin. *Journal of Geophysical Research* 92 (B), 9385–9406.
- Collins, A.S., 2006. Madagascar and the amalgamation of Central Gondwana. *Gondwana Research* 9, 3–16.
- Collins, A.S., Windley, B.F., 2002. The tectonic evolution of central and northern Madagascar and its place in the final assembly of Gondwana. *Journal of Geology* 110, 325–339.
- Coltice, N., Phillips, B.R., Bertrand, H., Ricard, Y., Rey, P., 2007. Global warming of the mantle at the origin of flood basalts over supercontinents. *Geology* 35, 391–394.
- Coltice, N., Bertrand, H., Rey, P., Jourdan, F., Phillips, B.R., Ricard, Y., 2009. Global warming of the mantle beneath continents back to the Archaean. *Gondwana Research* 15, 254–266.
- Cotten, J., Le Dez, A., Bau, M., Caroff, M., Maury, R.C., Dulsky, P., Yfrcade, S., Bohn, M., Brousse, R., 1995. Origin of anomalous rare-earth element and yttrium enrichments in subaerially exposed basalts: evidence from French Polynesia. *Chemical Geology* 119, 115–138.
- Cox, K.G., 1988. The Karoo Province. In: Macdougall, J.D. (Ed.), *Continental Flood Basalts*. Kluwer Academic, Netherlands, pp. 239–271.
- De Wit, M.J., 1999. Alex du Toit special issue. *Gondwana-10, event stratigraphy of Gondwana*, keynote presentations: *Journal of African Earth Sciences*, vol. 28, pp. 1–277.
- De Wit, M.J., 2003. Madagascar: heads it's a continent, tails it's an island. *Annual Review of Earth and Planetary Sciences* 31, 213–248.
- De Wit, M.J., Bowring, S.A., Ashwal, L.D., Rangeloson, R.A., Morel, V.P.I., Randrianasolo, L.G., 1998. Tectonics of Neoproterozoic ductile shear zones in southwestern Madagascar, with implications for Gondwana studies, addendum to extended abstracts, *Gondwana - 10, event stratigraphy of Gondwana*, 10th International Conference, Cape Town, South Africa, June 28–July 4, 1998. *Journal of African Earth Sciences* 27 (1A), II–III.
- Deckart, K., Bertrand, H., Liégeois, J.P., 2005. Geochemistry and Sr, Nd, Pb isotopic composition of the Central Atlantic Magmatic Province (CAMP) in Guyana and Guinea. *Lithos* 82, 289–314.
- Deniel, C., 1988. Geochemical and isotopic (Sr, Nd, Pb) evidence for plume–lithosphere interactions in the genesis of Grande Comore magmas (Indian Ocean). *Chemical Geology* 144, 281–303.
- DePaolo, D.J., 1981. Neodymium isotopes in the Colorado Front Range and crust–mantle evolution in the Proterozoic. *Nature* 291, 193–196.
- DePaolo, D.J., 1983. The mean life of continents: estimates of continent recycling rates from Nd and Hf isotopic data and implications for mantle structure. *Geophysical Research Letters* 10, 705–708.
- Dostal, J., Dupuy, C., Nicollet, C., Cantagrel, J.M., 1992. Geochemistry and petrogenesis of Upper Cretaceous basaltic rocks from southern Malagasy. *Chemical Geology* 97 (3–4), 199–218.
- Dumoulin, C., Doin, M.P., Arcay, Floutout, L., 2004. Onset of small-scale instabilities at the base of the lithosphere: scaling laws and role of pre-existing lithospheric structures. *Geophysical Journal International* 160, 344–356.
- Duncan, A.R., Erlank, A.J., Marsh, J.S., 1984. Regional geochemistry of the Karoo igneous province. In: Erlank, A.J. (Ed.), *Petrogenesis of the Volcanic Rocks of the Karoo Province: Special Publication of the Geological Society of South Africa*, vol. 13, pp. 355–388.
- Duncan, R.A., Backman, J., Peterson, L., 1989. Reunion hotspot activity through tertiary time: initial results from the Ocean Drilling Program, Leg 115. *Journal of Volcanology and Geothermal Research* 36, 193–198.
- Emerick, C.M., Duncan, R.A., 1982. Age progressive volcanism in the Comore Archipelago, western Indian Ocean and implications for Somali plate tectonics. *Earth and Planetary Science Letters* 60, 415–428 and errata, 1983, 62, 439.
- Ewart, A., Milner, S.C., Armstrong, R.A., Duncan, A.R., 1998. Etendeka volcanism of the Goboboseb Mountains and Messum igneous complex, Namibia. Part I: geochemical evidence of early cretaceous Tristan Plume melts and the role of crustal contamination in the Paraná–Etendeka CFB. *Journal of Petrology* 39 (2), 191–225.
- Gastal, M.P., Lafon, J.M., Hartmann, L.A., Koester, E., 2005. Sm–Nd isotopic investigation of Neoproterozoic and Cretaceous igneous rocks from southern Brazil: a study of magmatic processes. *Lithos* 82, 345–377.
- Geiger, M., Clark, D.N., Mette, W., 2004. Reappraisal of the timing of the breakup of Gondwana based on sedimentological and seismic evidence from the Morondava Basin, Madagascar. *Journal of African Earth Sciences* 38 (4), 363–381.
- Gioan, P., Rasendrasoa, J., Bardintzeff, J.M., Rasamimanana, G., 1996. Nouvelles données pétrographiques et structurales sur le magmatisme du Sud du bassin de Morondava (Sud-Ouest de Madagascar). *Journal of African Earth Sciences* 22 (4), 597–608.
- Hawkesworth, C.J., Gallagher, K., 1993. Mantle hotspots, plumes and regional tectonics as causes of intraplate magmatism. *Terra Nova* 5, 552–559.
- Hawkesworth, C., Kelley, S., Turner, S., Le Roex, A., Storey, B., 1999. Mantle processes during Gondwana break-up and dispersal. *Journal of African Earth Sciences* 28, 239–261.
- Hofmann, A.W., Jochum, K.P., 1996. Source characteristics derived from very incompatible trace elements in Mauna Loa and Mauna Kea basalts, Hawaii scientific drilling project. *Journal of Geophysical Research* 101 (B5), 11831–11839.
- Jourdan, F., Bertrand, H., Féraud, G., Le Gall, B., Watkeys, M.K., 2009. Lithospheric mantle evolution monitored by overlapping large igneous provinces: case study in southern Africa. *Lithos* 107, 257–268.
- Karceh, J.P., 1973. Le massif volcanique d'Ambre et les régions voisines de Madagascar. *Etude volcanologique et pétrologique. Annales Sciences Université Besançon*, vol. 19, 173 pp.
- King, S.D., Anderson, D.L., 1998. Edge-driven convection. *Earth and Planetary Science Letters* 160, 289–296.
- Kröner, A., Windley, B.F., Jaekel, P., Brewer, T.S., Razakamanana, T., 1999. New zircon ages and regional significance for the evolution of the Pan-African orogen in Madagascar. *Journal of the Geological Society of London* 156, 1125–1135.
- Kröner, A., Hegner, E., Collins, A.S., Windley, B.F., Brewer, T.S., Razakamanana, T., Pidgeon, R.T., 2000. Age and magmatic history of the Antananarivo block, Central Madagascar, as derived from zircon geochronology and Nd isotopic systematics. *American Journal of Science* 300, 251–288.
- Kusky, T.M., Toraman, E., Raharimahefa, T., 2007. The Great Rift Valley of Madagascar: an extension of the Africa–Somali diffuse plate boundary? *Gondwana Research* 11, 577–579.
- Lacroix, A., 1916. La constitution des roches volcaniques de l'Extrême Nord de Madagascar et de Nosy Bé; les ankaratrites de Madagascar en général. *Comptes Rendus Académie des Sciences, Paris* 163, 253–258.
- Le Maitre, R.W. (Ed.), 2002. *Igneous Rocks, A Classification and Glossary of Terms*. (Recommendations of the International Union of Geological Sciences Subcommittee on the Systematics of Igneous Rocks). Cambridge University Press, Cambridge, UK.
- Liégeois, J.P., Sauvage, J.F., Black, R., 1991. The Permo-Jurassic alkaline Province of Tadhak, Mali: geology, geochronology and tectonic significance. *Lithos* 27, 95–105.
- Liégeois, J.P., Navez, J., Hertogen, J., Black, R., 1998. Contrasting origin of post-collisional high-K calc-alkaline and shoshonitic versus alkaline and peralkaline granitoids. *Lithos* 45, 1–28.
- Liégeois, J.P., Latouche, L., Boughrara, M., Navez, J., Guiraud, M., 2003. The LATEA metacraton (Central Hoggar, Tuareg shield, Algeria): behaviour of an old passive margin during the Pan-African orogeny. *Journal of African Earth Sciences* 37, 161–190.
- Liégeois, J.P., Benhallou, A., Azzouni-Sekkal, A., Yahiaoui, R., Bonin, B., 2005. The Hoggar swell and volcanism: reactivation of the Precambrian Tuareg shield during Alpine convergence and West African Cenozoic volcanism. In: Foulger, G.R., Natland, J.H., Presnall, D.C., Anderson, D.L. (Eds.), *Plates, Plumes and Paradigms: Geological Society of America Special Paper*, vol. 388, pp. 379–400.
- Ludwig, K.R., 2003. *Isoplot 3.00, a geochronological toolkit for Microsoft Excel: Berkeley Geochronology Center Special Publication*, vol. 4, 69 pp.
- Lugmair, G.W., Marti, K., 1978. Lunar initial $^{143}\text{Nd}/^{144}\text{Nd}$: differential evolution of the lunar crust and mantle. *Earth and Planetary Science Letters* 39, 349–357.
- Macdonald, G.A., Katsura, T., 1964. Chemical composition of Hawaiian lavas. *Journal of Petrology* 5, 82–133.
- Mahoney, J., Nicollet, C., Dupuy, C., 1991. Madagascar basalts: tracking oceanic and continental sources. *Earth and Planetary Science Letters* 104, 350–363.
- Mahoney, J.J., le Roex, A.P., Peng, Z.X., Fisher, R.L., Natland, J.H., 1992. Southwestern limits of Indian ocean ridge mantle and the origin of low $^{206}\text{Pb}/^{204}\text{Pb}$ mid-ocean ridge basalt: isotope systematics of the central Southwest Indian Ridge (17–50°E). *Journal of Geophysical Research* 97, 19771–19790.
- Mahoney, J.J., Saunders, A.D., Storey, M., Randriamanantenasoa, A., 2008. Geochemistry of the Volcan de l'Androy Basalt–Rhyolite Complex, Madagascar Cretaceous Igneous Province. *Journal of Petrology* 49 (6), 1069–1096.
- Mahood, G.A., Drake, R.E., 1982. K–Ar dating young rhyolitic rocks: a case study of the Sierra La Primavera, Jalisco, Mexico. *Geological Society of America Bulletin* 93, 1232–1241.
- Marks, K.M., Tikku, A.A., 2001. Cretaceous reconstructions of East Antarctica, Africa and Madagascar. *Earth and Planetary Science Letters* 186, 479–495.
- Maruyama, S., Santosh, M., Zhao, D., 2007. Superplume, supercontinent, and post-perovskite: mantle dynamics and anti-plate tectonics on the core–mantle boundary. *Gondwana Research* 11, 7–37.
- McKenzie, D., Bickle, M.J., 1988. The volume and composition of melt generated by extension of the lithosphere. *Journal of Petrology* 29, 625–680.
- Meert, J.G., Lieberman, B.S., 2008. The Neoproterozoic assembly of Gondwana and its relationship to the Ediacaran–Cambrian radiation. *Gondwana Research* 14, 5–21.
- Meert, J.G., Tamrat, E., 2006. Paleomagnetic evidence for a stationary Marion hotspot: additional paleomagnetic data from Madagascar. *Gondwana Research* 10, 340–348.
- Meibom, A., Anderson, D.L., 2003. The statistical upper mantle assemblage. *Earth and Planetary Science Letters* 217, 123–139.
- Melluso, L., Morra, V., 2000. Petrogenesis of Late Cenozoic mafic alkaline rocks of the Nosy Be archipelago (northern Madagascar): relationships with the Comorean magmatism. *Journal of Volcanology and Geothermal Research* 96, 129–142.
- Melluso, L., Morra, V., Brotzu, P., Razafiniparany, A., Ratriimo, V., Razafimahatratra, D., 1997. Geochemistry and Sr-isotopic composition of the late cretaceous flood basalt sequence of northern Madagascar: petrogenetic and geodynamic implications. *Journal of African Earth Sciences* 24 (3), 371–390.
- Melluso, L., Morra, V., Brotzu, P., Mahoney, J.J., 2001. The Cretaceous igneous province of Madagascar: geochemistry and petrogenesis of lavas and dykes from the central-western sector. *Journal of Petrology* 42 (7), 1249–1278.
- Melluso, L., Morra, V., Brotzu, P., D'Antonio, M., Bennio, L., 2002. Petrogenesis of the Late Cretaceous Tholeiitic magmatism in the passive margins of northeastern Madagascar. In: Menzies, M.A., Klemperer, S.L., Ebinger, C.J., Baker, J. (Eds.), *Volcanic Rifted Margins: Geological Society of America Special Paper*, vol. 362, pp. 83–98.

- Melluso, L., Morra, V., Brotzu, P., Franciosi, L., Lieberknecht, A.M.P., Bennio, L., 2003. Geochemical provinciality in the Cretaceous basaltic magmatism of Northern Madagascar: mantle source implications. *Journal of the Geological Society of London* 160 (3), 477–488.
- Melluso, L., Morra, V., Brotzu, P., Tommasini, S., Renna, M.R., Duncan, R.A., Franciosi, L., D'Amelio, F., 2005. Geochronology and petrogenesis of the Cretaceous Antampombato–Ambatovy Complex and associated dyke swarm, Madagascar. *Journal of Petrology* 46 (10), 1963–1996.
- Melluso, L., Morra, V., Riziky, H., Veloson, J., Lustrino, M., Del Gatto, L., Modeste, V., 2007. Petrogenesis of a basanite–tephrite–phonolite volcanic suite in the Bobaomy (Cap d'Ambre) Peninsula, northern Madagascar. *Journal of African Earth Sciences* 49 (1–2), 29–42.
- Melluso, L., Sheth, H.C., Mahoney, J.J., Morra, V., Petrone, C.M., Storey, M., 2009. Correlations between silicic volcanic rocks of the St Mary's Islands (southwestern India) and eastern Madagascar: implications for Late Cretaceous India–Madagascar reconstructions. *Journal of the Geological Society of London* 166, 283–294.
- Nelson, B.K., DePaolo, D.J., 1985. Rapid production of continental crust 1.7 to 1.9 b.y. ago: Nd isotopic evidence from the basement of the North American midcontinent. *Geological Society of America Bulletin* 96, 746–754.
- Nicolas, A., Boudier, F., 2008. Large shear zones with no relative displacement. *Terra Nova* 20, 200–205.
- Nicollet, C., 1984. Le volcanisme dans le Sud-Ouest de Madagascar. *Journal of African Earth Sciences* 2 (4), 383–388.
- Nougier, J., Cantagrel, J.M., Karche, J.P., 1986. The Comores archipelago in the western Indian Ocean: volcanology, geochronology and geodynamic setting. *Journal of African Earth Sciences* 5, 135–145.
- Odin, G.S., Hunziker, J.C., 1982. Radiometric dating of the Albian–Cenomanian boundary. In: Odin, G.S. (Ed.), *Numerical Dating Stratigraphy*. John Wiley and Sons Ltd, pp. 537–556.
- O'Neill, C., Lenardic, A., Jellinek, A.M., Moresi, L., 2009. Influence of supercontinents on deep mantle flow. *Gondwana Research*. doi:10.1016/j.gr.2008.11.005.
- Pande, K., Sheth, H.C., Bhutani, R., 2001. 40Ar–39Ar age of the St. Mary's Islands volcanics, southern India: record of India–Madagascar break-up on the Indian subcontinent. *Earth and Planetary Science Letters* 193 (1–2), 39–46.
- Papini, M., Benvenuti, M., 2008. The Toarcian–Bathonian succession of the Antsiranana Basin (NW Madagascar): facies analysis and tectono-sedimentary history in the development of the East Africa–Madagascar conjugate margins. *Journal of African Earth Sciences* 51 (1), 21–38.
- Paquette, J.L., Nédelec, A., Moine, B., Rakotondrazafy, M., 1994. U–Pb, single zircon Pb–evaporation, and Sm–Nd isotopic study of a granulite domain in SE Madagascar. *Journal of Geology* 102 (5), 523–538.
- Patriat, P., Achache, J., 1984. India–Eurasia collision chronology has implications for crustal shortening and driving mechanism of plates. *Nature* 311, 615–621.
- Pearce, J.A., 1983. The role of sub-continental lithosphere in magma genesis at destructive plate margins. In: Hawkesworth, C.J., Norry, M.J. (Eds.), *Continental Basalts and Mantle Xenoliths*, pp. 230–249. Nantwich, Shiva.
- Piqué, A., Bardintzeff, J.M., Bellon, H., Bignot, G., Brousse, R., Chorowicz, J., Chotin, P., Gioan, P., Laville, E., Plaziat, J.C., Rahaingoarivony, G., Rakotondraompiana, S., Rakotondrazafy, R., Rasamimanana, G., Razafindrazaka, Y., Réhault, J.P., Thouin, C., Randriamananjara, T., Rasendrasoa, J., Rabarimanana, M.H., Ravololonirina, Y., Tidahy, E., 1999. L'évolution géologique de Madagascar et la dislocation du Gondwana: une introduction. *Journal of African Earth Sciences* 28 (4), 919–930.
- Raillard, S., 1990. Les marges de l'Afrique de l'Est et les zones de fractures associées. Chaîne Davie et ride du Mozambique. Campagne MD-60 / MACAMO II, Thèse de Doctorat en Sciences de l'Université Pierre et Marie Curie, Paris, 272 p.
- Rakotondrazafy, A.F., Nedelec, A., Guilianni, G., 2007. Incipient charnockitisation triggered by structurally-controlled CO₂ influx in central Madagascar. *Gondwana Research* 11, 584–585.
- Rakotosolofa, N.A., Torsvik, T.H., Ashwall, L.D., Eide, E.A., De Wit, M.J., 1999. The Karoo Supergroup revisited and Madagascar–Africa fits. *Journal of African Earth Sciences* 29 (1), 135–151.
- Rasamimanana, G., 1996. Caractérisations géochimiques et géochronologiques de trois épisodes magmatiques (Crétacé, Miocène terminal et Quaternaire) à Madagascar, associés aux phénomènes de rifting. Thèse de Doctorat en Sciences de l'Université de Paris-Sud, Orsay, 234 p.
- Rasamimanana, G., Bardintzeff, J.M., Rasendrasoa, J., Bellon, H., Thouin, C., Gioan, P., Piqué, A., 1998. Les épisodes magmatiques du Sud-Ouest de Madagascar (bassin de Morondava) marqueurs des phénomènes de rifting crétacé et néogène. *Comptes Rendus Académie des Sciences*, Paris 326, 685–691.
- Rino, S., Kon, Y., Sato, W., Maruyama, S., Santosh, M., Zhao, D., 2008. The Grenvillian and Pan-African orogens: world's largest orogenies through geological time, and their implication on the origin of superplume. *Gondwana Research* 14, 51–72.
- Rolin, P., 1991. Présence de décrochements précambriens dans le bouclier méridional de Madagascar: implications structurales et géodynamiques. *Comptes Rendus Académie des Sciences*, Paris 312, 625–629.
- Rotstein, Y., Munsch, M., Bernard, A., 2001. The Kerguelen Province revisited: additional constraints on the early development of the Southeast Indian Ocean. *Marine Geophysical Researches* 22, 81–100.
- Santosh, M., Maruyama, S., Yamamoto, S., 2009. The making and breaking of supercontinents: some speculations based on superplume, superdownwelling and the role of tectosphere. *Gondwana Research* 16, 324–341.
- Schandelmeier, H., Bremer, F., Holl, H.G., 2004. Kinematic evolution of the Morondava rift basin of SW Madagascar – from wrench tectonics to normal extension. *Journal of African Earth Sciences* 38 (4), 321–330.
- Schettino, A., Scotese, C.R., 2005. Apparent polar wander paths for the major continents (200 Ma to the present day): a palaeomagnetic reference frame for global plate tectonic reconstructions. *Geophysical Journal International* 163, 727–759.
- Shackleton, R.M., 1996. The final collision between East and West Gondwana: where is it? *Journal of African Earth Sciences* 23 (3), 271–287.
- Späth, A., le Roex, A.P., Duncan, R.A., 1996. The geochemistry of lavas from the Comores archipelago, Western Indian Ocean: petrogenesis and mantle source region characteristics. *Journal of Petrology* 37, 961–991.
- Stampfli, G.M., Borel, G.D., 2002. A plate tectonic model for the Paleozoic and Mesozoic constrained by dynamic plate boundaries and restored synthetic oceanic isochrons. *Earth and Planetary Science Letters* 196, 17–33.
- Steiger, R.H., Jäger, E., 1977. Subcommission on geochronology: convention on the use of decay constants in geo- and cosmochronology. *Earth and Planetary Science Letters* 36, 359–362.
- Stern, R.J., 2002. Crustal evolution in the East African Orogen: a neodymium isotopic perspective. *Journal of African Earth Sciences* 34, 109–117.
- Storey, M., Mahoney, J.J., Saunders, A.D., Duncan, R.A., Kelley, S.P., Coffin, M.F., 1995. Timing of hot spot-related volcanism and the breakup of Madagascar and India. *Science* 267, 852–855.
- Storey, M., Mahoney, J.J., Saunders, A.D., 1997. Cretaceous basalts in Madagascar and the transition between plume and continental lithosphere mantle sources. In: Mahoney, J.J., Coffin, M.F. (Eds.), *Large Igneous Provinces: Continental, Oceanic, and Planetary Flood Volcanism*. : Geophysical Monograph, vol. 100. American Geophysical Union, pp. 95–122.
- Storey, B.C., Rubridge, B.S., Cole, D.I., de Wit, M.J. (Eds.), 2000a. Special Issue, Gondwana-10, Event Stratigraphy of Gondwana Proceedings: *Journal of African Earth Sciences*, vol. 29, p. 1.
- Storey, B.C., de Wit, M.J., Anderson, J.M., Anderson, H.M., Rubridge, B.S., Thomas, R.J. (Eds.), 2000b. Special Issue, Gondwana-10, Event Stratigraphy of Gondwana Proceedings, volume 2: *Journal of African Earth Sciences*, vol. 31, p. 1.
- Stracke, A., Hofman, A.W., Hart, S.R., 2005. FOZO, HIMU, and the rest of the mantle zoo. *Geochemistry Geophysics Geosystems* 6 (5), Q05007. doi:10.1029/2004GC000824.
- Sun, S.S., McDonough, W.F., 1989. Chemical and isotopic systematics of oceanic basalts: implications for mantle composition and processes. In: Saunders, A.D., Norry, M.J. (Eds.), *Magmatism in the Ocean Basins: Geological Society of London Special Publication*, pp. 313–345.
- Teyssier, C., Tikoff, B., 1998. Strike-slip partitioned transpression of the San Andreas fault system: a lithospheric-scale approach. In: Holdsworth, A., Strachan, B., Dewey, C. (Eds.), *Continental Transpressional and Transensional Tectonics: Geological Society of London Special Publication*, vol. 135, pp. 143–158.
- Tingey, D.G., Christiansen, E.H., Best, M.G., Ruiz, J., Lux, D.R., 1991. Tertiary minette and melanephelinite dikes, Wasatch Plateau, Utah: records of mantle heterogeneities and changing tectonics. *Journal of Geophysical Research* 96 (B8), 13529–13544.
- Tucker, R.D., Ashwal, L.D., Handke, M.J., Hamilton, M.A., Le Grange, M., Rambeloson, R.A., 1999. U–Pb geochronology and isotope geochemistry of the Archean and Proterozoic rocks of North-Central Madagascar. *Journal of Geology* 107 (2), 135–153.
- Tucker, R.D., Kuksy, T.M., Buchwaldt, R., Handke, M.J., 2007. Neoproterozoic nappes and superposed folding of the Itremo Group, west-central Madagascar. *Gondwana Research* 12, 356–379.
- Vogt, M., Kröner, A., Poller, U., Sommer, H., Muhongo, S., Wingate, M.T.D., 2006. Archean and Palaeoproterozoic gneisses reworked during a Neoproterozoic (Pan-African) high-grade event in the Mozambique belt of East Africa: structural relationships and zircon ages from the Kidatu area, central Tanzania. *Journal of African Earth Sciences* 45, 139–155.
- Weaver, B.L., 1991a. Trace element evidence for the origin of ocean-island basalts. *Geology* 19, 123–126.
- Weaver, B.L., 1991b. The origin of ocean island basalt end-member compositions: trace element and isotopic constraints. *Earth and Planetary Science Letters* 104, 381–397.
- Wedepohl, K.H., 1991. Chemical composition and fractionation of the continental crust. *Geologische Rundschau* 80, 207–223.
- Wedepohl, K.H., 1995. The composition of the continental crust. *Geochimica et Cosmochimica Acta* 59, 1217–1232.
- White, W.M., 1995. Geochemical tracers of mantle processes. *Reviews of Geophysics*, supp., U.S. Nat. Rep. to Int. Union of geodesy and geophysics 1991–1994. American Geophysical Union, pp. 19–24.
- Whittington, A.G., Hofmeister, A.M., Nabelek, P.I., 2009. Temperature-dependent thermal diffusivity of the Earth's crust and implications for magmatism. *Nature* 458, 319–321.
- Wilson, M., 1989. *Igneous petrogenesis, a global tectonic approach*. Unwin Hyman, London.
- Yin, A., 2006. Cenozoic tectonic evolution of the Himalayan orogen as constrained by along-strike variation of structural geometry, exhumation history, and foreland sedimentation. *Earth Science Reviews* 76, 1–131.
- Yoshida, M., Rajesh, H.M., Santosh, M., 1999. Juxtaposition of India and Madagascar: a perspective. *Gondwana Research* 2, 449–462.
- Zhu, B., 2007. Pb–Sr–Nd isotopic systematics of mantle-derived rocks in the world. *Earth Science Frontiers* 14 (2), 24–36.
- Zindler, A., Hart, S.R., 1986. Chemical geodynamics. *Annual Review of Earth and Planetary Sciences* 86 (14), 493–571.